Chapter 3
Collective Periodic Motion Coordination

This chapter introduces a collective periodic motion coordination problem. Coordinated periodic motions play an important role in applications involving multi-agent networks with repetitive movements such as cooperative patrol, mapping, sampling, or surveillance. We introduce two types of algorithms. For the first type, we introduce Cartesian coordinate coupling to existing distributed consensus algorithms for respectively, single-integrator dynamics and double-integrator dynamics, to generate collective motions, namely, rendezvous, circular patterns, and logarithmic spiral patterns in the three-dimensional space. It is shown that the interaction graph and the value of the Euler angle in the case of single-integrator dynamics and the interaction graph, the damping gain, and the value of the Euler angle in the case of double-integrator dynamics affect the resulting collective motions. We show that when the nonsymmetric Laplacian matrix has certain properties, the damping gain is above a certain bound in the case of double-integrator dynamics, and the Euler angle is below, equal, or above a critical value, the agents will eventually rendezvous, move on circular orbits, or follow logarithmic spiral curves lying on a plane normal to the Euler axis. For the second type, we introduce coupled second-order linear harmonic oscillators with local interaction to generate synchronized oscillatory motions. We analyze convergence conditions under, respectively, directed fixed and switching interaction graphs. It is shown that the coupled harmonic oscillators can be synchronized under mild network connectivity conditions. The theoretical result is also applied to synchronized motion coordination in multi-agent systems as a proof of concept.

3.1 Cartesian Coordinate Coupling

In this section, we introduce Cartesian coordinate coupling to existing distributed consensus algorithms for respectively, single-integrator dynamics and double-integrator dynamics, through a rotation matrix in the three-dimensional space, analyze the convergence properties, and quantitatively characterize the resulting collective

W. Ren, Y. Cao, *Distributed Coordination of Multi-agent Networks*,
Communications and Control Engineering,
DOI 10.1007/978-0-85729-169-1_3,

motions, namely, convergence to a point, circular patterns with concentric orbits, and logarithmic spiral curves lying on a plane normal to the Euler axis, under a general interaction graph. The resulting collective motions are expected to have applications in rendezvous, persistent surveillance, and coverage control with teams of heterogeneous agents. It is shown that the interaction graph and the value of the Euler angle in the case of single-integrator dynamics and the interaction graph, the damping gain, and the value of the Euler angle in the case of double-integrator dynamics affect the resulting collective motions. The analysis relies on algebraic graph theory, matrix theory, and properties of the Kronecker product.

3.1.1 Single-integrator Dynamics

Consider n agents with single-integrator dynamics given by

$$\dot{r}_i = u_i, \quad i = 1, \ldots, n, \tag{3.1}$$

where $r_i \in \mathbb{R}^m$ is the position and $u_i \in \mathbb{R}^m$ is the control input associated with the ith agent. We introduce a distributed algorithm with Cartesian coordinate coupling for (3.1) as

$$u_i = -\sum_{j=1}^{n} a_{ij} C(r_i - r_j), \quad i = 1, \ldots, n, \tag{3.2}$$

where a_{ij} is the (i, j)th entry of the adjacency matrix $\mathcal{A} \in \mathbb{R}^{n\times n}$ associated with the directed graph $\mathcal{G} \triangleq (\mathcal{V}, \mathcal{E})$ characterizing the interaction among the n agents, and $C \in \mathbb{R}^{m\times m}$ denotes a Cartesian coordinate coupling matrix. In this book, it is assumed that all agents share a common inertial coordinate frame. This assumption will not be explicitly mentioned in later chapters unless it is necessary for facilitating analysis. In this section, we focus on the case where C is a rotation matrix while a similar analysis can be extended to the case where C is a general matrix.

Remark 3.1 Note that the existing consensus algorithm for (3.1) (see e.g., [248, Chap. 2]) corresponds to the case where $C = I_m$. That is, using the existing consensus algorithm for (3.1), the components of r_i (i.e., the Cartesian coordinates of agent i) are decoupled while using (3.2) the components of r_i are coupled.

Using (3.2), (3.1) can be written in a vector form as

$$\dot{r} = -(\mathcal{L} \otimes C)r, \tag{3.3}$$

where $r \triangleq [r_1^T, \ldots, r_n^T]^T$ and $\mathcal{L} \in \mathbb{R}^{n\times n}$ is the nonsymmetric Laplacian matrix associated with $\mathcal{A}$ and hence $\mathcal{G}$. Before moving on, we need the following definition:

Definition 3.1. Let μ_i, $i = 1, \ldots, n$, be the ith eigenvalue of $-\mathcal{L}$ with an associated right eigenvector w_i and an associated left eigenvector ν_i. Also let $\arg(\mu_i) = 0$ for

$\mu_i = 0$ and $\arg(\mu_i) \in (\frac{\pi}{2}, \frac{3\pi}{2})$ for all $\mu_i \neq 0$.[1] Without loss of generality, suppose that μ_i is labeled such that $\arg(\mu_1) \leq \arg(\mu_2) \leq \cdots \leq \arg(\mu_n)$.[2]

Theorem 3.2. *Suppose that the directed graph $\mathcal{G}$ has a directed spanning tree. Let the control algorithm for (3.1) be given by (3.2), where $r_i \triangleq [x_i, y_i, z_i]^T$ and C is the 3×3 rotation matrix R defined in Lemma 1.20. Let μ_i, w_i, ν_i, and $\arg(\mu_i)$ be defined in Definition 3.1, $\mathbf{p} \in \mathbb{R}^n$ be defined in Lemma 1.1, and $\mathbf{a} \triangleq [a_1, a_2, a_3]^T$, ς_k, and ϖ_k be defined in Lemma 1.20.*

1. *If $|\theta| < \theta_s^c$, where $\theta_s^c \triangleq \frac{3\pi}{2} - \arg(\mu_n)$, the agents will eventually rendezvous at the position $[\mathbf{p}^T x(0), \mathbf{p}^T y(0), \mathbf{p}^T z(0)]$, where x, y, and z are, respectively, the column stack vectors of x_i, y_i, and z_i.*
2. *If $|\theta| = \theta_s^c$ and $\arg(\mu_n)$ is the unique maximum phase of μ_i, all agents will eventually move on circular orbits with the center $[\mathbf{p}^T x(0), \mathbf{p}^T y(0), \mathbf{p}^T z(0)]$ and the period $\frac{2\pi}{|\mu_n|}$. The radius of the orbit for agent i is given by $2|w_{n(i)}(\frac{\nu_n^T}{\nu_n^T w_n} \otimes \frac{\varpi_2^T}{\varpi_2^T \varsigma_2})r(0)|\sqrt{a_2^2 + a_3^2}\sin^2(\frac{\theta}{2})$, where $w_{n(i)}$ is the ith component of w_n. The relative radius of the orbits is equal to the relative magnitude of $w_{n(i)}$. The relative phase of the agents on their orbits is equal to the relative phase of $w_{n(i)}$. The circular orbits are on a plane normal to the Euler axis $\mathbf{a}$.*
3. *If $\arg(\mu_n)$ is the unique maximum phase of μ_i and $\theta_s^c < |\theta| < \frac{3\pi}{2} - \arg(\mu_{n-1})$, all agents will eventually move along logarithmic spiral curves with the center $[\mathbf{p}^T x(0), \mathbf{p}^T y(0), \mathbf{p}^T z(0)]$, the growing rate $|\mu_n|\cos(\arg(\mu_n) + |\theta|)$, and the period $\frac{2\pi}{|\mu_n \sin(\arg(\mu_n)+|\theta|)|}$. The radius of the logarithmic spiral curve for agent i is given by*

$$2\left|w_{n(i)}\left(\frac{\nu_n^T}{\nu_n^T w_n} \otimes \frac{\varpi_2^T}{\varpi_2^T \varsigma_2}\right) r(0)\right| e^{[|\mu_n|\cos(\arg(\mu_n)+|\theta|)]t} \sqrt{a_2^2 + a_3^2}\sin^2\left(\frac{\theta}{2}\right).$$

The relative radius of the logarithmic spiral curves is equal to the relative magnitude of $w_{n(i)}$. The relative phase of the agents on their curves is equal to the relative phase of $w_{n(i)}$. The logarithmic spiral curves are on a plane normal to the Euler axis $\mathbf{a}$.

Proof: It follows from Lemmas 1.20 and 1.21 and Definition 3.1 that the eigenvalues of $-(\mathcal{L} \otimes R)$ are μ_i, $\mu_i e^{\iota\theta}$, and $\mu_i e^{-\iota\theta}$ with the associated right eigenvectors $w_i \otimes \varsigma_1$, $w_i \otimes \varsigma_2$, and $w_i \otimes \varsigma_3$, respectively, and the associated left eigenvectors $\nu_i \otimes \varpi_1$, $\nu_i \otimes \varpi_2$, and $\nu_i \otimes \varpi_3$, respectively. That is, the eigenvalues of $-(\mathcal{L} \otimes R)$ correspond to the eigenvalues of $-\mathcal{L}$ rotated by angles 0, θ, and $-\theta$, respectively. Let λ_ℓ, $\ell = 1, \ldots, 3n$, denote the ℓth eigenvalue of $-(\mathcal{L} \otimes R)$. Without loss of generality, let $\lambda_{3i-2} = \mu_i$, $\lambda_{3i-1} = \mu_i e^{\iota\theta}$, and $\lambda_{3i} = \mu_i e^{-\iota\theta}$, $i = 1, \ldots, n$. Because the directed graph $\mathcal{G}$ has a directed spanning tree, it follows from Lemma 1.1 that $-\mathcal{L}$ has a

[1] Note that according to Lemma 1.1, $-\mathcal{L}$ has at least one zero eigenvalue and all its nonzero eigenvalues have negative real parts.

[2] It follows from Lemma 1.1 that $\mu_1 = 0$. Without loss of generality, let $w_1 = \mathbf{1}_n$ and $\nu_1 = \mathbf{p}$, where $\mathbf{p} \in \mathbb{R}^n$ is defined in Lemma 1.1.

simple zero eigenvalue and all other eigenvalues have negative real parts. According to Definition 3.1, we let $\mu_1 = 0$ and $\mathrm{Re}(\mu_i) < 0$, $i = 2, \ldots, n$. According to Lemma 1.1, we let $w_1 = \mathbf{1}_n$ and $\nu_1 = \mathbf{p}$ without loss of generality. Because $\mu_1 = 0$ and $\mu_i \neq 0, i = 2, \ldots, n$, it follows that $-(\mathcal{L} \otimes R)$ has exactly three zero eigenvalues (i.e., $\lambda_1 = \lambda_2 = \lambda_3 = 0$).

Note that $-(\mathcal{L} \otimes R)$ can be written in the Jordan canonical form as MJM^{-1}, where the columns of M, denoted by m_k, $k = 1, \ldots, 3n$, can be chosen to be the right eigenvectors or generalized right eigenvectors of $-(\mathcal{L} \otimes R)$ associated with the eigenvalue λ_k, the rows of M^{-1}, denoted by p_k^T, $k = 1, \ldots, 3n$, can be chosen to be the left eigenvectors or generalized left eigenvectors of $-(\mathcal{L} \otimes R)$ associated with the eigenvalue λ_k such that $p_k^T m_k = 1$ and $p_k^T m_\ell = 0$, $k \neq \ell$, and J is the Jordan block diagonal matrix with λ_k being the diagonal entries. Noting that $\lambda_k = 0$, $k = 1, 2, 3$, we can choose $m_k = \mathbf{1}_n \otimes \varsigma_k$ and $p_k = \mathbf{p} \otimes \frac{\varpi_k}{\varpi_k^T \varsigma_k}$, $k = 1, 2, 3$. Note that $e^{-(\mathcal{L} \otimes R)t} = Me^{Jt}M^{-1}$. Also note that $\lim_{t \to \infty} e^{J_\ell t} = 0_{q \times q}$ when $J_\ell \in \mathbb{R}^{q \times q}$ is a Jordan block corresponding to an eigenvalue with a negative real part.

For the first statement of the theorem, note that $\mu_1 = 0$ and $\mathrm{Re}(\mu_i) < 0$, $i = 2, \ldots, n$. Also note from Definition 3.1 that $\arg(\mu_\mathrm{i}) \in [\arg(\mu_2), \arg(\mu_\mathrm{n})] \subset (\frac{\pi}{2}, \frac{3\pi}{2})$, $i = 2, \ldots, n$. Noting that all complex eigenvalues of $-\mathcal{L}$ are in conjugate pairs, it follows that $\arg(\mu_2) = 2\pi - \arg(\mu_\mathrm{n})$. If $|\theta| < \theta_s^c$, then all $\arg(\mu_\mathrm{i})$, $\arg(\mu_\mathrm{i} \mathrm{e}^{\boldsymbol{\iota}\theta})$, and $\arg(\mu_\mathrm{i} \mathrm{e}^{-\boldsymbol{\iota}\theta})$ are within $(\frac{\pi}{2}, \frac{3\pi}{2})$, $i = 2, \ldots, n$, which implies that $\mathrm{Re}(\lambda_\ell) < 0$, $\ell = 4, \ldots, 3n$. Noting that $\lambda_k = 0$, $k = 1, 2, 3$, it follows that $\lim_{t \to \infty} r(t) = \lim_{t \to \infty} e^{-(\mathcal{L} \otimes R)t} r(0) = (\sum_{k=1}^3 m_k p_k^T) r(0) = (\mathbf{1}_n \mathbf{p}^T \otimes I_3) r(0)$. It thus follows that $x_i(t) \to \mathbf{p}^T x(0)$, $y_i(t) \to \mathbf{p}^T y(0)$, and $z_i(t) \to \mathbf{p}^T z(0)$ as $t \to \infty$. That is, all agents will eventually rendezvous at $[\mathbf{p}^T x(0), \mathbf{p}^T y(0), \mathbf{p}^T z(0)]$.

For the second statement of the theorem, if $\theta = \theta_s^c$ (respectively, $\theta = -\theta_s^c$), then μ_n rotated by an angle θ (respectively, $-\theta$) will locate on the imaginary axis, that is, $\lambda_{3n-1} = \mu_n e^{\boldsymbol{\iota}\theta} = -|\mu_n| \boldsymbol{\iota}$ (respectively, $\lambda_{3n} = \mu_n e^{-\boldsymbol{\iota}\theta} = -|\mu_n| \boldsymbol{\iota}$), while $\mu_2 = \overline{\mu_n}$ rotated by an angle $-\theta$ (respectively, θ) will also locate on the imaginary axis, that is, $\lambda_6 = \mu_2 e^{-\boldsymbol{\iota}\theta} = |\mu_n| \boldsymbol{\iota}$ (respectively, $\lambda_5 = \mu_2 e^{\boldsymbol{\iota}\theta} = |\mu_n| \boldsymbol{\iota}$). Because $\arg(\mu_n)$ is the unique maximum phase of μ_i, λ_{3n-1} (respectively, λ_{3n}) and λ_6 (respectively, λ_5) are the only two nonzero eigenvalues of $-(\mathcal{L} \otimes R)$ on the imaginary axis and all other nonzero eigenvalues have negative real parts. In the following, we focus on $\theta = \theta_s^c$ since the analysis for $\theta = -\theta_s^c$ is similar except that the agents will move in reverse directions. Note that $\lambda_k = 0$, $k = 1, 2, 3$, and $\mathrm{Re}(\lambda_\ell) < 0$ for all $\ell \neq 1, 2, 3, 3n - 1, 6$. Noting that $\lambda_{3n-1} = -|\mu_n| \boldsymbol{\iota}$ and $\lambda_6 = |\mu_n| \boldsymbol{\iota}$, we can choose $m_{3n-1} = w_n \otimes \varsigma_2$, $p_{3n-1} = \frac{\nu_n}{\nu_n^T w_n} \otimes \frac{\varpi_2}{\varpi_2^T \varsigma_2}$, $m_6 = \overline{m_{3n-1}}$, and $p_6 = \overline{p_{3n-1}}$. Note that $r(t) = e^{-(\mathcal{L} \otimes R)t} r(0)$. It follows that $\|r(t) - (\sum_{k=1}^3 m_k p_k^T + e^{-\boldsymbol{\iota}|\mu_n|t} m_{3n-1} p_{3n-1}^T + e^{\boldsymbol{\iota}|\mu_n|t} m_6 p_6^T) r(0)\| \to 0$ as $t \to \infty$. Define $c(t) \triangleq (e^{-\boldsymbol{\iota}|\mu_n|t} m_{3n-1} p_{3n-1}^T + e^{\boldsymbol{\iota}|\mu_n|t} m_6 p_6^T) r(0)$. Let $c_k(t)$ be the kth component of $c(t)$, $k = 1, \ldots, 3n$. It follows that $c_{3(i-1)+\ell}(t) = 2\mathrm{Re}(e^{-\boldsymbol{\iota}|\mu_n|t} w_{n(i)} \varsigma_{2(\ell)} p_{3n-1}^T r(0))$, where $i = 1, \ldots, n$, $\ell = 1, 2, 3$, and $\varsigma_{2(\ell)}$ denotes the ℓth component of ς_2. After some manipulation, it follows that $c_{3(i-1)+\ell}(t) = 2|\varsigma_{2(\ell)} w_{n(i)} p_{3n-1}^T r(0)| \times \cos\{|\mu_n| t - \arg[w_{n(i)} p_{3n-1}^T r(0)] - \arg[\varsigma_{2(\ell)}]\}$, $i = 1, \ldots, n$, $\ell = 1, 2, 3$. Therefore, it follows that $\|x_i(t) - [\mathbf{p}^T x(0) + c_{3i-2}(t)]\| \to 0$, $\|y_i(t) - [\mathbf{p}^T y(0) +$

$c_{3i-1}(t)]\| \to 0$, and $\|z_i(t) - [\mathbf{p}^T z(0) + c_{3i}(t)]\| \to 0$ as $t \to \infty$. After some manipulation, it can be verified that $\|[c_{3i-2}(t), c_{3i-1}(t), c_{3i}(t)]^T\| = 2|w_{n(i)} p_{3n-1}^T \times r(0)|\sqrt{a_2^2 + a_3^2 \sin^2(\frac{\theta}{2})}$, which is a constant. It thus follows that all agents will eventually move on circular orbits with the center $[\mathbf{p}^T x(0), \mathbf{p}^T y(0), \mathbf{p}^T z(0)]$ and the period $\frac{2\pi}{|\mu_n|}$. The radius of the orbit for agent i is given by $2|w_{n(i)} p_{3n-1}^T r(0)| \times \sqrt{a_2^2 + a_3^2 \sin^2(\frac{\theta}{2})}$. Note that the relative radius of the orbits is equal to the relative magnitude of $w_{n(i)}$. In addition, it is straightforward to see that the relative phase of the agents on their orbits is equal to the relative phase of $w_{n(i)} p_{3n-1}^T r(0)$, which is equivalent to the relative phase of $w_{n(i)}$. Note from Lemma 1.20 that the Euler axis $\mathbf{a}$ is orthogonal to both $\mathrm{Re}(\varsigma_2)$ and $\mathrm{Im}(\varsigma_2)$, where $\mathrm{Re}(\cdot)$ and $\mathrm{Im}(\cdot)$ are applied componentwise. It can thus be verified that $\mathbf{a}$ is orthogonal to $[c_{3i-2}(t), c_{3i-1}(t), c_{3i}(t)]^T$, which implies that the circular orbits are on a plane normal to $\mathbf{a}$.

For the third statement of the theorem, if $\arg(\mu_n)$ is the unique maximum phase of μ_i and $\theta_s^c < \theta < \frac{3\pi}{2} - \arg(\mu_{n-1})$ (respectively, $\arg(\mu_{n-1}) - \frac{3\pi}{2} < \theta < -\theta_s^c$), then μ_n rotated by an angle θ (respectively, $-\theta$) will have a positive real part, that is, $\lambda_{3n-1} = \mu_n e^{\boldsymbol{\iota}\theta} = |\mu_n| e^{\boldsymbol{\iota}(\arg(\mu_n)+\theta)}$ (respectively, $\lambda_{3n} = \mu_n e^{-\boldsymbol{\iota}\theta} = |\mu_n| e^{\boldsymbol{\iota}[\arg(\mu_n)-\theta]}$), while $\mu_2 = \overline{\mu_n}$ rotated by an angle $-\theta$ (respectively, θ) will also have a positive real part, that is, $\lambda_6 = \mu_2 e^{-\boldsymbol{\iota}\theta} = |\mu_n| e^{-\boldsymbol{\iota}(\arg(\mu_n)+\theta)}$ (respectively, $\lambda_5 = \mu_2 e^{\boldsymbol{\iota}\theta} = |\mu_n| e^{-\boldsymbol{\iota}[\arg(\mu_n)-\theta]}$). In addition, λ_{3n-1} (respectively, λ_{3n}) and λ_6 (respectively, λ_5) are the only two eigenvalues of $-(\mathcal{L} \otimes R)$ with positive real parts and all other nonzero eigenvalues have negative real parts. In the following, we focus on $\theta_s^c < \theta < \frac{3\pi}{2} - \arg(\mu_{n-1})$ since the analysis for $\arg(\mu_{n-1}) - \frac{3\pi}{2} < \theta < -\theta_s^c$ is similar except that all agents will move in reverse directions. Note that $\lambda_k = 0$, $k = 1, 2, 3$, $\mathrm{Re}(\lambda_{3n-1}) > 0$, $\mathrm{Re}(\lambda_6) > 0$, and $\mathrm{Re}(\lambda_k) < 0$ otherwise. Similar to the proof of the second statement, define $c(t) \triangleq \{e^{|\mu_n| e^{\boldsymbol{\iota}(\arg(\mu_n)+\theta)} t} m_{3n-1} p_{3n-1}^T + e^{|\mu_n| e^{-\boldsymbol{\iota}[\arg(\mu_n)+\theta]} t} m_6 p_6^T\} r(0)$. Let $c_k(t)$, $k = 1, \ldots, 3n$, be the kth component of $c(t)$. Also let $\varrho_i = |w_{n(i)} p_{3n-1}^T r(0)|$ and $\varphi_i = \arg[w_{n(i)} p_{3n-1}^T r(0)]$. It follows that $\|x_i(t) - [\mathbf{p}^T x(0) + c_{3i-2}(t)]\| \to 0$, $\|y_i(t) - [\mathbf{p}^T y(0) + c_{3i-1}(t)]\| \to 0$, and $\|z_i(t) - [\mathbf{p}^T z(0) + c_{3i}(t)]\| \to 0$ as $t \to \infty$, where

$$c_{3(i-1)+\ell}(t) = 2|\varsigma_{2(\ell)}| \varrho_i e^{\{|\mu_n| \cos[\arg(\mu_n)+\theta]\}t} \times \cos\big(\big\{|\mu_n| \sin[\arg(\mu_n) + \theta]\big\}t + \varphi_i + \arg[\varsigma_{2(\ell)}]\big),$$

$i = 1, \ldots, n$, $\ell = 1, 2, 3$. Similar to the argument for the second statement, it can be verified that

$$\big\|\big[c_{3i-2}(t), c_{3i-1}(t), c_{3i}(t)\big]^T\big\| = 2\varrho_i e^{\{|\mu_n| \cos[\arg(\mu_n)+\theta]\}t} \sqrt{a_2^2 + a_3^2} \sin^2\left(\frac{\theta}{2}\right),$$

which is growing with time. It thus follows that all agents will eventually move along logarithmic spiral curves. The statement then follows directly. ■

Corollary 3.1. *Suppose that the directed graph $\mathcal{G}$ has a directed spanning tree. Let the control algorithm for (3.1) be given by (3.2), where $r_i \triangleq [x_i, y_i]^T$ and C is the 2×2 rotation matrix given by $R(\theta) \triangleq \left[\begin{smallmatrix} \cos(\theta) & \sin(\theta) \\ -\sin(\theta) & \cos(\theta) \end{smallmatrix}\right]$.*

1. *If* $|\theta| < \theta_s^c$, *where* $\theta_s^c \triangleq \frac{3\pi}{2} - \arg(\mu_n)$, *the agents will eventually rendezvous at the position* $[\mathbf{p}^T x(0), \mathbf{p}^T y(0)]$, *where* x *and* y *are, respectively, the column stack vectors of* x_i *and* y_i, *and* $\mathbf{p} \in \mathbb{R}^n$ *is defined in Lemma* 1.1.
2. *If* $|\theta| = \theta_s^c$ *and* $\arg(\mu_n)$ *is the unique maximum phase of* μ_i, *all agents will eventually move on circular orbits with the center* $[\mathbf{p}^T x(0), \mathbf{p}^T y(0)]$ *and the period* $\frac{2\pi}{|\mu_n|}$. *The radius of the orbit for agent* i *is given by* $2|w_{n(i)}(\frac{\nu_n^T}{\nu_n^T w_n} \otimes [\frac{1}{2}, -\frac{1}{2}\boldsymbol{\iota}])r(0)|$. *The relative radius of the orbits is equal to the relative magnitude of* $w_{n(i)}$. *The relative phase of the agents on their orbits is equal to the relative phase of* $w_{n(i)}$.
3. *If* $\arg(\mu_n)$ *is the unique maximum phase of* μ_i *and* $\theta_s^c < |\theta| < \frac{3\pi}{2} - \arg(\mu_{n-1})$, *all agents will eventually move along logarithmic spiral curves with the center* $[\mathbf{p}^T x, \mathbf{p}^T y]$, *the growing rate* $|\mu_n| \cos[\arg(\mu_n) + |\theta|]$, *and the period* $\frac{2\pi}{|\mu_n \sin[\arg(\mu_n)+|\theta|]|}$. *The radius of the logarithmic spiral curve for agent* i *is given by*

$$2\left|w_{n(i)}\left(\frac{\nu_n^T}{\nu_n^T w_n} \otimes \left[\frac{1}{2}, -\frac{1}{2}\boldsymbol{\iota}\right]\right) r(0)\right| e^{\{|\mu_n| \cos[\arg(\mu_n)+|\theta|]\}t}.$$

The relative radius of the logarithmic spiral curves is equal to the relative magnitude of $w_{n(i)}$. *The relative phase of the agents on their curves is equal to the relative phase of* $w_{n(i)}$.

Proof: The eigenvalues of $R(\theta)$ are given by $e^{\boldsymbol{\iota}\theta}$ and $e^{-\boldsymbol{\iota}\theta}$, with the associated right eigenvectors $[1, \boldsymbol{\iota}]^T$ and $[1, -\boldsymbol{\iota}]^T$ and left eigenvectors $[1, -\boldsymbol{\iota}]^T$ and $[1, \boldsymbol{\iota}]^T$, respectively. The rest of the proof follows from that of Theorem 3.2. ■

Corollary 3.2. *Suppose that the directed graph* $\mathcal{G}$ *is a unidirectional ring (i.e., a cyclic pursuit graph). Also suppose that* $a_{ij} = 1$ *if* $(j, i) \in \mathcal{E}$ *and* $a_{ij} = 0$ *otherwise. Let the control algorithm for* (3.1) *be given by* (3.2), *where* r_i *and* C *are given as in Corollary* 3.1.

1. *If* $|\theta| < \frac{\pi}{n}$, *the agents will eventually rendezvous at the position* $[\mathbf{p}^T x(0), \mathbf{p}^T y(0)]$, *where* x, y, *and* $\mathbf{p}$ *are defined in Corollary* 3.1.
2. *If* $|\theta| = \frac{\pi}{n}$, *all agents will eventually move on the same circular orbit with the center* $[\mathbf{p}^T x(0), \mathbf{p}^T y(0)]$, *the period* $\frac{\pi}{\sin(\frac{\pi}{n})}$, *and the radius* $2|w_{n(i)}(\frac{\nu_n^T}{\nu_n^T w_n} \otimes [\frac{1}{2}, -\frac{1}{2}\boldsymbol{\iota}])r(0)|$.[3] *In addition, all agents will eventually be evenly distributed on the orbit.*
3. *If* $\frac{\pi}{n} < |\theta| < \frac{2\pi}{n}$, *all agents will eventually move along logarithmic spiral curves with the center* $[\mathbf{p}^T x(0), \mathbf{p}^T y(0)]$, *the growing rate* $2\sin(\frac{\pi}{n})\sin(|\theta| - \frac{\pi}{n})$, *the period* $\frac{\pi}{\sin(\pi/n)\cos(|\theta|-\pi/n)}$, *and the radius* $2|w_{n(i)}(\frac{\nu_n^T}{\nu_n^T w_n} \otimes [\frac{1}{2}, -\frac{1}{2}\boldsymbol{\iota}])r(0)| \times e^{2[\sin(\frac{\pi}{n})\sin(|\theta|-\frac{\pi}{n})]t}$. *In addition, the phases of all agents will eventually be evenly distributed.*

Proof: Note that if $\mathcal{G}$ is a unidirectional ring and $a_{ij} = 1$ if $(j, i) \in \mathcal{E}$ and $a_{ij} = 0$ otherwise, then $\mathcal{L}$ is a circulant matrix. Also note that a circulant matrix can be

[3] In this case, all $w_{n(i)}$, $i = 1, \ldots, n$, have the same magnitude.

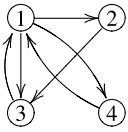

Fig. 3.1 Interaction graph for four agents. An *arrow* from j to i denotes that agent j is a neighbor of agent i

diagonalized by a Fourier matrix. The proof then follows Corollary 3.1 directly by use of the properties of the eigenvalues of a circulant matrix and the properties of the Fourier matrix. ■

Remark 3.3 Note that when $\mathcal{G}$ is a unidirectional ring (i.e., a cyclic pursuit graph) but different positive weights are chosen for a_{ij}, where $(j,i) \in \mathcal{E}$, all agents will move on orbits with different radii and their phases will not be evenly distributed.

Example 3.1. To illustrate, consider four agents with the directed graph $\mathcal{G}$ shown by Fig. 3.1. Let $\mathcal{L}$ associated with $\mathcal{G}$ be given by

$$\begin{bmatrix} 1.5 & 0 & -1.1 & -0.4 \\ -1.2 & 1.2 & 0 & 0 \\ -0.1 & -0.5 & 0.6 & 0 \\ -1 & 0 & 0 & 1 \end{bmatrix}. \tag{3.4}$$

It can be computed that $\theta_s^c = \frac{3\pi}{2} - \arg(\mu_4) = 1.2975$ rad, where $\mu_4 = -1.6737 - 0.4691\boldsymbol{\iota}$ and $\arg(\mu_4) \in (\pi, \frac{3\pi}{2})$. Let R be the rotation matrix corresponding to the Euler axis $\mathbf{a} = \frac{1}{14}[1,2,3]^T$ and the Euler angle $\theta = \theta_s^c$. Figures 3.2, 3.3, and 3.4 show, respectively, the eigenvalues of $-\mathcal{L}$ and $-(\mathcal{L} \otimes R)$ when $\theta = \theta_s^c - 0.1$, $\theta = \theta_s^c$, and $\theta = \theta_s^c + 0.1$. Note that the eigenvalues of $-(\mathcal{L} \otimes R)$ correspond to the eigenvalues of $-\mathcal{L}$ rotated by angles 0, θ, and $-\theta$. Note that in Fig. 3.2, all nonzero eigenvalues of $-(\mathcal{L} \otimes R)$ are in the open left half plane. In Fig. 3.3, the eigenvalues of $-(\mathcal{L} \otimes R)$ corresponding to μ_4 rotated by an angle θ and $\mu_2 = \overline{\mu_4}$ rotated by an angle $-\theta$ are located on the imaginary axis while all other nonzero eigenvalues are located in the open left half plane. In Fig. 3.4, the eigenvalues of $-(\mathcal{L} \otimes R)$ corresponding to μ_4 rotated by an angle θ and $\mu_2 = \overline{\mu_4}$ rotated by an angle $-\theta$ are located in the open right half plane while all other nonzero eigenvalues are located in the open left half plane.

3.1.2 Double-integrator Dynamics

Consider n agents with double-integrator dynamics given by

$$\dot{r}_i = v_i, \qquad \dot{v}_i = u_i, \quad i = 1, \ldots, n, \tag{3.5}$$

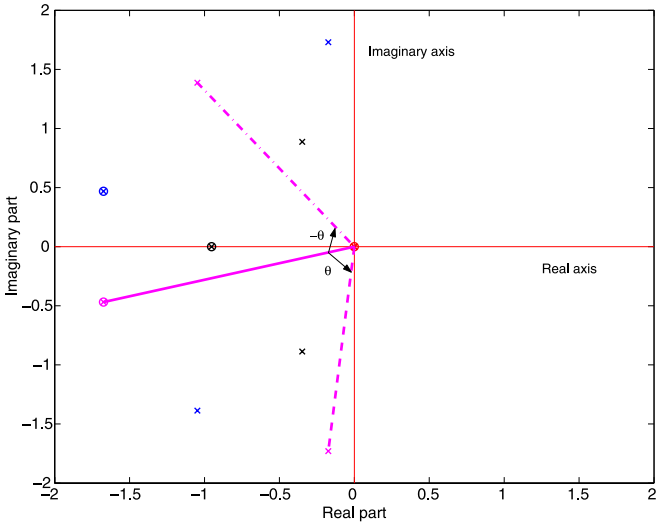

Fig. 3.2 Eigenvalues of $-\mathcal{L}$ and $-(\mathcal{L} \otimes R)$ with $\theta = \theta_s^c - 0.1$. *Circles* denote the eigenvalues of $-\mathcal{L}$ while x-marks denote the eigenvalues of $-(\mathcal{L} \otimes R)$. The eigenvalues of $-(\mathcal{L} \otimes R)$ correspond to the eigenvalues of $-\mathcal{L}$ rotated by angles 0, θ, and $-\theta$, respectively. In particular, the eigenvalues obtained by rotating μ_4 by angles 0, θ, and $-\theta$ are shown by, respectively, the *solid line*, the *dashed line*, and the *dashdot line*. Because $\theta < \theta_s^c$, all nonzero eigenvalues of $-(\mathcal{L} \otimes R)$ are in the *open left half plane*

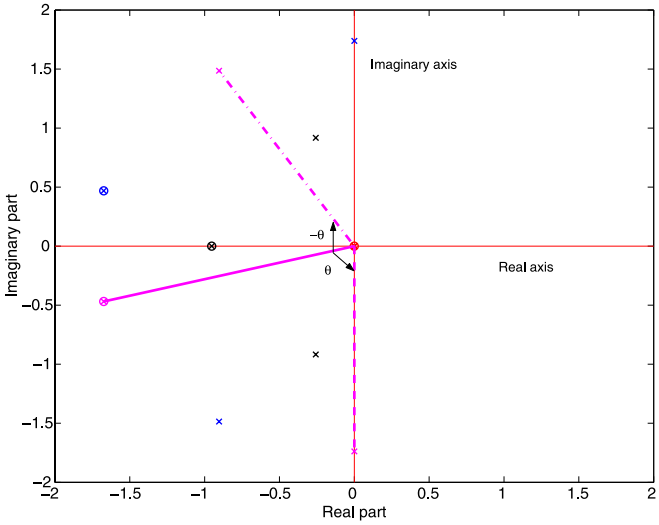

Fig. 3.3 Eigenvalues of $-\mathcal{L}$ and $-(\mathcal{L} \otimes R)$ with $\theta = \theta_s^c$. *Circles* denote the eigenvalues of $-\mathcal{L}$ while x-marks denote the eigenvalues of $-(\mathcal{L} \otimes R)$. The eigenvalues of $-(\mathcal{L} \otimes R)$ correspond to the eigenvalues of $-\mathcal{L}$ rotated by angles 0, θ, and $-\theta$, respectively. In particular, the eigenvalues obtained by rotating μ_4 by angles 0, θ, and $-\theta$ are shown by, respectively, the *solid line*, the *dashed line*, and the *dashdot line*. Because $\theta = \theta_s^c$, two nonzero eigenvalues of $-(\mathcal{L} \otimes R)$ are on the *imaginary axis*

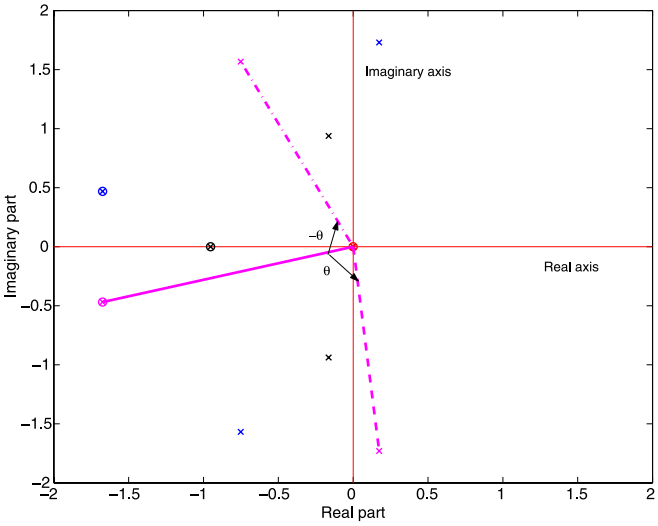

Fig. 3.4 Eigenvalues of $-\mathcal{L}$ and $-(\mathcal{L} \otimes R)$ with $\theta = \theta_s^c + 0.1$. *Circles* denote the eigenvalues of $-\mathcal{L}$ while x-marks denote the eigenvalues of $-(\mathcal{L} \otimes R)$. The eigenvalues of $-(\mathcal{L} \otimes R)$ correspond to the eigenvalues of $-\mathcal{L}$ rotated by angles 0, θ, and $-\theta$, respectively. In particular, the eigenvalues obtained by rotating μ_4 by angles 0, θ, and $-\theta$ are shown by, respectively, the *solid line*, the *dashed line*, and the *dashdot line*. Because $\theta > \theta_s^c$, two nonzero eigenvalues of $-(\mathcal{L} \otimes R)$ are in the *open right half plane*

where $r_i \in \mathbb{R}^m$ and $v_i \in \mathbb{R}^m$ are, respectively, the position and velocity of the ith agent, and $u_i \in \mathbb{R}^m$ is the control input. We introduce a distributed algorithm with Cartesian coordinate coupling for (3.5) as

$$u_i = -\sum_{j=1}^{n} a_{ij} C(r_i - r_j) - \alpha v_i, \quad i = 1, \ldots, n, \tag{3.6}$$

where a_{ij} is defined as in (3.2), $C \in \mathbb{R}^{m \times m}$ denotes a Cartesian coordinate coupling matrix, and α is a positive constant. In this section, we focus on the case where C is a rotation matrix while a similar analysis can be extended to the case where C is a general matrix.

Remark 3.4 Note that the existing consensus algorithm for (3.5) (see, e.g., [248, Chap. 4]) corresponds to the case where $C = I_m$. That is, using the existing consensus algorithm for (3.5), the components of r_i (i.e., the Cartesian coordinates of agent i) are decoupled while using (3.6) the components of r_i are coupled.

Before moving on, we need the following lemma.

Lemma 3.1. *Let ξ_i be the ith eigenvalue of $A \in \mathbb{R}^{n \times n}$ with, respectively, an associated right eigenvector q_i and an associated left eigenvector s_i. Also let $B \triangleq \begin{bmatrix} 0_{n \times n} & I_n \\ A & -\alpha I_n \end{bmatrix}$, where α is a positive scalar. Then the eigenvalues of B are*

given by $\zeta_{2i-1} = \frac{-\alpha+\sqrt{\alpha^2+4\xi_i}}{2}$ *with, respectively, the associated right and left eigenvectors* $\left[\begin{smallmatrix} q_i \\ \zeta_{2i-1}q_i \end{smallmatrix}\right]$ *and* $\left[\begin{smallmatrix} (\zeta_{2i-1}+\alpha)s_i \\ s_i \end{smallmatrix}\right]$ *and* $\zeta_{2i} = \frac{-\alpha-\sqrt{\alpha^2+4\xi_i}}{2}$*, with, respectively, the associated right and left eigenvectors given by* $\left[\begin{smallmatrix} q_i \\ \zeta_{2i}q_i \end{smallmatrix}\right]$ *and* $\left[\begin{smallmatrix} (\zeta_{2i}+\alpha)s_i \\ s_i \end{smallmatrix}\right]$*. When* $\mathrm{Re}(\xi_i) < 0$*,* $\mathrm{Re}(\zeta_{2i-1}) < 0$ *and* $\mathrm{Re}(\zeta_{2i}) < 0$ *if and only if* $\alpha > \frac{|\mathrm{Im}(\xi_i)|}{\sqrt{\mathrm{Re}(-\xi_i)}}$.

Proof: For the first statement, suppose that ζ is an eigenvalue of B with an associated right eigenvector $\left[\begin{smallmatrix} f \\ g \end{smallmatrix}\right]$, where $f, g \in \mathbb{C}^n$. It follows that $\left[\begin{smallmatrix} 0_{n\times n} & I_n \\ A & -\alpha I_n \end{smallmatrix}\right]\left[\begin{smallmatrix} f \\ g \end{smallmatrix}\right] = \zeta\left[\begin{smallmatrix} f \\ g \end{smallmatrix}\right]$, which implies $g = \zeta f$ and $Af - \alpha g = \zeta g$. It thus follows that $Af = (\zeta^2 + \alpha\zeta)f$. Noting that $Aq_i = \xi_i q_i$, we let $f = q_i$ and $\zeta^2 + \alpha\zeta = \xi_i$. That is, each eigenvalue of A, ξ_i, corresponds to two eigenvalues of B, denoted by $\zeta_{2i-1,2i} = \frac{-\alpha\pm\sqrt{\alpha^2+4\xi_i}}{2}$. Because $g = \zeta f$, it follows that the right eigenvectors associated with ζ_{2i-1} and ζ_{2i} are, respectively, $\left[\begin{smallmatrix} q_i \\ \zeta_{2i-1}q_i \end{smallmatrix}\right]$ and $\left[\begin{smallmatrix} q_i \\ \zeta_{2i}q_i \end{smallmatrix}\right]$. A similar analysis can be used to find the left eigenvectors of B associated with ζ_{2i-1} and ζ_{2i}.

For the second statement, note that $\sqrt{\alpha^2 + 4\xi_i}$ has a nonnegative real part. Because $\zeta_{2i} = \frac{-\alpha-\sqrt{\alpha^2+4\xi_i}}{2}$, it follows that $\mathrm{Re}(\zeta_{2i}) < 0$ if $\alpha > 0$. It is left to show the conditions under which $\mathrm{Re}(\zeta_{2i-1}) < 0$. Suppose that α_i^* is the critical value for α such that ζ_{2i-1} is on the imaginary axis. Let $\zeta_{2i-1} = \eta_i \boldsymbol{\imath}$, where $\eta_i \in \mathbb{R}$. After some manipulation, it follows that $\alpha_i^* = \frac{|\mathrm{Im}(\xi_i)|}{\sqrt{\mathrm{Re}(-\xi_i)}}$. Note that $\mathrm{Re}(\xi_i) < 0$. It is straightforward to verify that if $\alpha > \alpha_i^*$ (respectively, $\alpha < \alpha_i^*$), then ζ_{2i-1} has a negative (respectively, positive) real part. Therefore, when $\mathrm{Re}(\xi_i) < 0$, $\mathrm{Re}(\zeta_{2i-1}) < 0$ and $\mathrm{Re}(\zeta_{2i}) < 0$ if and only if $\alpha > \frac{|\mathrm{Im}(\xi_i)|}{\sqrt{\mathrm{Re}(-\xi_i)}}$. ■

Theorem 3.5. *Suppose that the directed graph* $\mathcal{G}$ *has a directed spanning tree. Let the control algorithm for* (3.5) *be given by* (3.6)*, where* $r_i \triangleq [x_i, y_i, z_i]^T$ *and* $v_i \triangleq [v_{xi}, v_{yi}, v_{zi}]^T$*. Let* μ_i*,* w_i*,* ν_i*, and* $\arg(\mu_i)$ *be defined in Definition* 3.1*,* $\mathbf{p} \in \mathbb{R}^n$ *be defined in Lemma* 1.1*, and* $\mathbf{a} \triangleq [a_1, a_2, a_3]^T$*,* ς_k*, and* ϖ_k *be defined in Lemma* 1.20*.*

1. *Suppose that* $C = I_3$*. Then all agents will eventually rendezvous if and only if* $\alpha > \alpha^c$*, where* $\alpha^c \triangleq \max_{\mu_i \neq 0} \frac{|\mathrm{Im}(\mu_i)|}{\sqrt{\mathrm{Re}(-\mu_i)}}$*. The rendezvous position is given by*

$$\left\{\mathbf{p}^T\left[x(0) + \frac{v_x(0)}{\alpha}\right], \mathbf{p}^T\left[y(0) + \frac{v_y(0)}{\alpha}\right], \mathbf{p}^T\left[z(0) + \frac{v_z(0)}{\alpha}\right]\right\}, \tag{3.7}$$

   where x*,* y*,* z*,* v_x*,* v_y*, and* v_z *are, respectively, column stack vectors of* x_i*,* y_i*,* z_i*,* v_{xi}*,* v_{yi}*, and* v_{zi}*.*
2. *Suppose that* $C = R$*, where* R *is the* 3×3 *rotation matrix defined in Lemma 1.20, and* $\alpha > \alpha^c$*. Given* $|\mu_i|$*,* $i = 2, \ldots, n$*, let* $\psi_i^l \in (\frac{\pi}{2}, \pi)$ *(respectively,* $\psi_i^u \in (\pi, \frac{3\pi}{2})$*) be the solution to* $|\mu_i| \sin^2(\psi_i) + \alpha^2 \cos(\psi_i) = 0$ *if* $\arg(\mu_i) \in (\frac{\pi}{2}, \pi]$ *(respectively,* $\arg(\mu_i) \in [\pi, \frac{3\pi}{2})$*). If* $|\theta| < \theta_d^c$*, where* $\theta_d^c \triangleq \min_{\arg(\mu_i)\in[\pi, \frac{3\pi}{2})}[\psi_i^u - \arg(\mu_i)]$*, then all agents will eventually rendezvous at the position given by* (3.7)*.*

3. *Under the assumption of part 2, if* $|\theta| = \theta_d^c$ *and there exists a unique* $\arg(\mu_\kappa) \in [\pi, \frac{3\pi}{2})$ *such that* $\psi_\kappa^u - \arg(\mu_\kappa) = \theta_d^c$, *then all agents will eventually move on circular orbits with the center given by* (3.7) *and the period* $\frac{\pi\alpha}{|\mu_\kappa \sin(\psi_\kappa^u)|}$. *The radius of the orbit for agent* i *is given by* $2|w_{\kappa(i)} p_c^T [r(0)^T, v(0)^T]^T| \sqrt{a_2^2 + a_3^2} \sin^2(\frac{\theta}{2})$, *where* $w_{\kappa(i)}$ *is the* i*th component of* w_κ *and*

$$p_c \triangleq \frac{1}{(2\sigma_c + \alpha)\nu_\kappa^T w_\kappa \varpi_2^T \varsigma_2} \begin{bmatrix} (\sigma_c + \alpha)(\nu_\kappa \otimes \varpi_2) \\ \nu_\kappa \otimes \varpi_2 \end{bmatrix},$$

where $\sigma_c \triangleq \boldsymbol{\iota} \frac{2|\mu_\kappa| \sin(\psi_\kappa^u)}{\alpha}$. *The relative radius of the orbits is equal to the relative magnitude of* $w_{\kappa(i)}$. *The relative phase of the agents on their orbits is equal to the relative phase of* $w_{\kappa(i)}$. *The circular orbits are on a plane normal to the Euler axis* $\mathbf{a}$.

4. *Under the assumption of part 2, if there exists a unique* $\arg(\mu_\kappa) \in [\pi, \frac{3\pi}{2})$ *such that* $\psi_\kappa^u - \arg(\mu_\kappa) = \theta_d^c$ *and* $\theta_d^c < |\theta| < \min_{\arg(\mu_i) \in [\pi, \frac{3\pi}{2}),\, i \neq \kappa} [\psi_i^u - \arg(\mu_i)]$, *then all agents will eventually move along logarithmic spiral curves with the center given by* (3.7), *the growing rate* $\mathrm{Re}(\sigma_s)$, *where* $\sigma_s \triangleq \frac{-\alpha + \sqrt{\alpha^2 + 4\lambda_s}}{2}$ *with* $\lambda_s \triangleq \mu_\kappa e^{\boldsymbol{\iota}|\theta|}$, *and the period* $\frac{2\pi}{|\mathrm{Im}(\sigma_s)|}$. *The radius of the logarithmic spiral curve for agent* i *is*

$$2|w_{\kappa(i)} p_s^T [r(0)^T, v(0)^T]^T e^{\mathrm{Re}(\sigma_s)t} \sqrt{a_2^2 + a_3^2} \sin^2\left(\frac{\theta}{2}\right),$$

where $p_s \triangleq \frac{1}{(2\sigma_s + \alpha)\nu_\kappa^T w_\kappa \varpi_2^T \varsigma_2} \left[\begin{smallmatrix} (\sigma_s + \alpha)(\nu_\kappa \otimes \varpi_2) \\ \nu_\kappa \otimes \varpi_2 \end{smallmatrix} \right]$. *The relative radius of the logarithmic spiral curves is equal to the relative magnitude of* $w_{\kappa(i)}$. *The relative phase of the agents on their curves is equal to the relative phase of* $w_{\kappa(i)}$. *The curves are on a plane normal to the Euler axis* $\mathbf{a}$.

Proof: For the first statement, if $C = I_3$, then (3.5) using (3.6) can be written in a vector form as

$$\begin{bmatrix} \dot{r} \\ \dot{v} \end{bmatrix} = \left(\underbrace{\begin{bmatrix} 0_{n\times n} & I_n \\ -\mathcal{L} & -\alpha I_n \end{bmatrix}}_{\Psi} \otimes I_3 \right) \begin{bmatrix} r \\ v \end{bmatrix}, \tag{3.8}$$

where $r \triangleq [r_1^T, \ldots, r_n^T]^T$ and $v \triangleq [v_1^T, \ldots, v_n^T]^T$. Note from Lemma 3.1 that each eigenvalue μ_i of $-\mathcal{L}$ corresponds to two eigenvalues of Ψ given by $\zeta_{2i-1} = \frac{-\alpha + \sqrt{\alpha^2 + 4\mu_i}}{2}$ with the associated right and left eigenvectors given by, respectively, $\left[\begin{smallmatrix} w_i \\ \zeta_{2i-1} w_i \end{smallmatrix} \right]$ and $\left[\begin{smallmatrix} (\zeta_{2i-1} + \alpha)\nu_i \\ \nu_i \end{smallmatrix} \right]$ and $\zeta_{2i} = \frac{-\alpha - \sqrt{\alpha^2 + 4\mu_i}}{2}$, with the associated right and left eigenvectors given by, respectively, $\left[\begin{smallmatrix} w_i \\ \zeta_{2i} w_i \end{smallmatrix} \right]$ and $\left[\begin{smallmatrix} (\zeta_{2i} + \alpha)\nu_i \\ \nu_i \end{smallmatrix} \right]$ where $i = 1, \ldots, n$. Because the directed graph $\mathcal{G}$ has a directed spanning tree, it follows from Lemma 1.1 that $-\mathcal{L}$ has a simple zero eigenvalue and all other eigenvalues have negative real parts. According to Definition 3.1, we let $\mu_1 = 0$ and $\mathrm{Re}(\mu_i) < 0$, $i = 2, \ldots, n$. According to Lemma 1.1, we let $w_1 = \mathbf{1}_n$ and $\nu_1 = \mathbf{p}$ without loss of

generality. It thus follows that $\zeta_1 = 0$[4] with the associated right and left eigenvectors given by, respectively, $\left[\begin{smallmatrix}\mathbf{1}_n\\ \mathbf{0}_n\end{smallmatrix}\right]$ and $\left[\begin{smallmatrix}\alpha\mathbf{p}\\ \mathbf{p}\end{smallmatrix}\right]$ and $\zeta_2 = -\alpha$.

We first show that the agents will eventually rendezvous at the position given by (3.7) if and only if Ψ defined in (3.8) has a simple zero eigenvalue and all other eigenvalues have negative real parts. For the sufficiency part, similar to the proof of Theorem 3.2, we write Ψ in the Jordan canonical form as $\Psi = MJM^{-1}$, where the columns of M, denoted by $m_k, k = 1, \ldots, 2n$, can be chosen to be the right eigenvectors or generalized right eigenvectors of Ψ associated with the eigenvalue ζ_k, the rows of M^{-1}, denoted by $p_k^T, k = 1, \ldots, 2n$, can be chosen to be the left eigenvectors or the generalized left eigenvectors of Ψ associated with eigenvalue ζ_k such that $p_k^T m_k = 1$ and $p_k^T m_\ell = 0$, $k \neq \ell$, and J is the Jordan block diagonal matrix with ζ_k being the diagonal entries. Noting that $\zeta_1 = 0$, we choose $m_1 = \left[\begin{smallmatrix}\mathbf{1}_n\\ \mathbf{0}_n\end{smallmatrix}\right]$ and $p_1 = \left[\begin{smallmatrix}\mathbf{p}\\ \frac{1}{\alpha}\mathbf{p}\end{smallmatrix}\right]$. Note that $e^{\Psi t} = Me^{Jt}M^{-1}$. Also note that $\lim_{t\to\infty} e^{J_\ell t} = 0_{q_\ell \times q_\ell}$ when $J_\ell \in \mathbb{R}^{q_\ell \times q_\ell}$ is a Jordan block corresponding to an eigenvalue with a negative real part. If Ψ has a simple zero eigenvalue and all other eigenvalues have negative real parts, then $\lim_{t\to\infty} e^{\Psi t} = M(\lim_{t\to\infty} e^{Jt})M^{-1} = \left[\begin{smallmatrix}\mathbf{1}_n\\ \mathbf{0}_n\end{smallmatrix}\right]\left[\begin{smallmatrix}\mathbf{p}^T & \frac{1}{\alpha}\mathbf{p}^T\end{smallmatrix}\right]$. It thus follows that

$$\lim_{t\to\infty}\begin{bmatrix} r(t)\\ v(t)\end{bmatrix} = \lim_{t\to\infty}(e^{\Psi t}\otimes I_3)\begin{bmatrix} r(0)\\ v(0)\end{bmatrix} = \left[\left(\begin{bmatrix}\mathbf{1}_n\\ \mathbf{0}_n\end{bmatrix}\begin{bmatrix}\mathbf{p}^T & \frac{1}{\alpha}\mathbf{p}^T\end{bmatrix}\right)\otimes I_3\right]\begin{bmatrix} r(0)\\ v(0)\end{bmatrix},$$

which implies that $x_i(t) \to \mathbf{p}^T x(0) + \frac{1}{\alpha}\mathbf{p}^T v_x(0)$, $y_i(t) \to \mathbf{p}^T y(0) + \frac{1}{\alpha}\mathbf{p}^T v_y(0)$, $z_i(t) \to \mathbf{p}^T z(0) + \frac{1}{\alpha}\mathbf{p}^T v_z(0)$, $v_{xi}(t) \to 0$, $v_{yi}(t) \to 0$, and $v_{zi}(t) \to 0$ as $t \to \infty$. Equivalently, it follows that all agents will eventually rendezvous at the position given by (3.7). For the necessity part, if the agents eventually rendezvous at the position given by (3.7), we know that $\lim_{t\to\infty} e^{\Psi t} = M(\lim_{t\to\infty} e^{Jt})M^{-1}$ has a rank one, which implies that $\lim_{t\to\infty} e^{Jt}$ has a rank one. Therefore, if the sufficient condition does not hold, it is easy to see that $\lim_{t\to\infty} e^{Jt}$ has a rank larger than one, which results in a contradiction.

We next show that Ψ has a simple zero eigenvalue and all other eigenvalues have negative real parts if and only if $\alpha > \alpha^c$. Note that $\zeta_2 < 0$ if $\alpha > 0$ because $\zeta_2 = -\alpha$. Because $\mathrm{Re}(\mu_i) < 0$, $i = 2, \ldots, n$, it follows from Lemma 3.1 that ζ_{2i-1} and ζ_{2i}, $i = 2, \ldots, n$, have negative real parts if and only if $\alpha > \frac{|\mathrm{Im}(\mu_i)|}{\sqrt{\mathrm{Re}(-\mu_i)}}$, $i = 2, \ldots, n$. Combining the above arguments shows that Ψ has a simple zero eigenvalue and all other eigenvalues have negative real parts if and only if $\alpha > \alpha^c$.

For the second statement, using (3.6), (3.5) can be written in a vector form as

$$\begin{bmatrix}\dot r\\ \dot v\end{bmatrix} = \underbrace{\begin{bmatrix} 0_{3n\times 3n} & I_{3n}\\ -(\mathcal{L}\otimes R) & -\alpha I_{3n}\end{bmatrix}}_{\Sigma}\begin{bmatrix} r\\ v\end{bmatrix}. \tag{3.9}$$

[4] Therefore, Ψ has at least one zero eigenvalue.

As in the proof of Theorem 3.2, let $\lambda_{3i-2} = \mu_i$, $\lambda_{3i-1} = \mu_i e^{\boldsymbol{\iota}\theta}$, and $\lambda_{3i} = \mu_i e^{-\boldsymbol{\iota}\theta}$, $i = 1, \ldots, n$, be the eigenvalues of $-(\mathcal{L} \otimes R)$. Note from Lemma 3.1 that each λ_k corresponds to two eigenvalues of Σ, defined in (3.9), given by $\sigma_{2k-1,2k} = \frac{-\alpha \pm \sqrt{\alpha^2 + 4\lambda_k}}{2}$, $k = 1, \ldots, 3n$. Because $\mu_1 = 0$, it follows that $\lambda_1 = \lambda_2 = \lambda_3 = 0$, which in turn implies that $\sigma_1 = \sigma_3 = \sigma_5 = 0$ and $\sigma_2 = \sigma_4 = \sigma_6 = -\alpha$. Because all $\sqrt{\alpha^2 + 4\lambda_k}$ have nonnegative real parts, it follows that all σ_{2k}, $k = 1, \ldots, 3n$, have negative real parts if $\alpha > 0$. Given $\alpha > 0$ and $\chi_i = |\mu_i| e^{\boldsymbol{\iota} \arg(\chi_i)}$, $i = 2, \ldots, n$, ψ_i^l and ψ_i^u are the critical values for $\arg(\chi_i) \in [0, 2\pi)$ such that $\frac{-\alpha + \sqrt{\alpha^2 + 4\chi_i}}{2}$ is on the imaginary axis. In particular, if $\arg(\chi_i) = \psi_i^l$ (respectively, ψ_i^u), then $\frac{-\alpha + \sqrt{\alpha^2 + 4\chi_i}}{2} = \boldsymbol{\iota} \frac{2|\mu_i| \sin(\arg(\psi_i^l))}{\alpha}$ (respectively, $\boldsymbol{\iota} \frac{2|\mu_i| \sin(\arg(\psi_i^u))}{\alpha}$), $i = 2, \ldots, n$. If $\arg(\chi_i) \in (\psi_i^l, \psi_i^u)$ (respectively, $\arg(\chi_i) \in [0, \psi_i^l) \cup (\psi_i^u, 2\pi)$), then $\frac{-\alpha + \sqrt{\alpha^2 + 4\chi_i}}{2}$ has negative (respectively, positive) real parts. Because $\alpha > \alpha^c$, the first statement implies that all $\frac{-\alpha + \sqrt{\alpha^2 + 4\mu_i}}{2}$, $i = 2, \ldots, n$, have negative real parts, which in turn implies that $\arg(\mu_i) \in (\psi_i^l, \psi_i^u)$, $i = 2, \ldots, n$. If $|\theta| < \theta_d^c$, then $\arg(\lambda_{3i-2})$, $\arg(\lambda_{3i-1})$, and $\arg(\lambda_{3i})$ are all within (ψ_i^l, ψ_i^u), which implies that σ_{6i-5}, σ_{6i-3}, and σ_{6i-1}, $i = 2, \ldots, n$, all have negative real parts. Therefore, if $|\theta| < \theta_d^c$, then Σ has exactly three zero eigenvalues and all other eigenvalues have negative real parts.

Similar to the proof of Theorem 3.2, we write Σ in the Jordan canonical form as MJM^{-1}, where the columns of M, denoted by m_k, $k = 1, \ldots, 6n$, can be chosen to be the right eigenvectors or generalized right eigenvectors of Σ associated with the eigenvalue σ_k, the rows of M^{-1}, denoted by p_k^T, $k = 1, \ldots, 6n$, can be chosen to be the left eigenvectors or generalized left eigenvectors of Σ associated with the eigenvalue σ_k such that $p_k^T m_k = 1$ and $p_k^T m_\ell = 0$, $k \neq \ell$, and J is the Jordan block diagonal matrix with σ_k being the diagonal entries. As in the proof of Theorem 3.2, the right and left eigenvectors of $-(\mathcal{L} \otimes R)$ associated with the eigenvalue $\lambda_\ell = 0$ are, respectively, $\mathbf{1}_n \otimes \varsigma_\ell$ and $\mathbf{p} \otimes \varpi_\ell$, where $\ell = 1, 2, 3$. It in turn follows from Lemma 3.1 that the right and left eigenvectors of Σ associated with $\sigma_{2\ell-1} = 0$ are, respectively, $\begin{bmatrix} \mathbf{1}_n \otimes \varsigma_\ell \\ \mathbf{0}_{3n} \end{bmatrix}$ and $\begin{bmatrix} \alpha \mathbf{p} \otimes \varpi_\ell \\ \mathbf{p} \otimes \varpi_\ell \end{bmatrix}$, where $\ell = 1, 2, 3$. We can choose $m_{2\ell-1} = \begin{bmatrix} \mathbf{1}_n \otimes \varsigma_\ell \\ \mathbf{0}_{3n} \end{bmatrix}$ and $p_{2\ell-1} = \begin{bmatrix} \mathbf{p} \otimes \frac{\varpi_\ell}{\varpi_\ell^T \varsigma_\ell} \\ \mathbf{p} \otimes \frac{\varpi_\ell}{\alpha \varpi_\ell^T \varsigma_\ell} \end{bmatrix}$, where $\ell = 1, 2, 3$. Note that $p_{2\ell-1}^T m_{2\ell-1} = 1$ and $p_{2\ell-1}^T m_{2k-1} = 0$, where $k, \ell = 1, 2, 3$ and $k \neq \ell$. Noting that $\sigma_{2\ell-1} = 0$, $\ell = 1, 2, 3$, it follows that $\lim_{t \to \infty} \begin{bmatrix} r(t) \\ v(t) \end{bmatrix} = (\lim_{t \to \infty} M e^{Jt} M^{-1}) \begin{bmatrix} r(0) \\ v(0) \end{bmatrix} = (\sum_{\ell=1}^3 m_{2\ell-1} p_{2\ell-1}^T) \begin{bmatrix} r(0) \\ v(0) \end{bmatrix}$, which implies that $x_i(t) \to \mathbf{p}^T x(0) + \frac{1}{\alpha} \mathbf{p}^T v_x(0)$, $y_i(t) \to \mathbf{p}^T y(0) + \frac{1}{\alpha} \mathbf{p}^T v_y(0)$, $z_i(t) \to \mathbf{p}^T z(0) + \frac{1}{\alpha} \mathbf{p}^T v_z(0)$, $v_{xi}(t) \to 0$, $v_{yi}(t) \to 0$, and $v_{zi}(t) \to 0$ as $t \to \infty$. Equivalently, it follows that all agents will eventually rendezvous at the position given by (3.7).

For the third statement, if $\theta = \theta_d^c$ (respectively, $\theta = -\theta_d^c$) and there exists a unique $\arg(\mu_\kappa) \in [\pi, \frac{3\pi}{2})$ such that $\psi_\kappa^u - \arg(\mu_\kappa) = \theta_d^c$, then $\lambda_{3\kappa-1} = \mu_\kappa e^{\boldsymbol{\iota}\theta} = |\mu_\kappa| e^{\boldsymbol{\iota}\psi_\kappa^u}$ (respectively, $\lambda_{3\kappa} = \mu_\kappa e^{-\boldsymbol{\iota}\theta} = |\mu_\kappa| e^{\boldsymbol{\iota}\psi_\kappa^u}$), which implies that $\sigma_{6\kappa-3} = \frac{-\alpha + \sqrt{\alpha^2 + 4\lambda_{3\kappa-1}}}{2} = \boldsymbol{\iota} \frac{2|\mu_\kappa| \sin(\psi_\kappa^u)}{\alpha}$ (respectively, $\sigma_{6\kappa-1} = \frac{-\alpha + \sqrt{\alpha^2 + 4\lambda_{3\kappa}}}{2} =$

$\boldsymbol{\iota}\frac{2|\mu_\kappa|\sin(\psi_\kappa^u)}{\alpha}$). Noting that the complex eigenvalues of Σ are in conjugate pairs, it follows that Σ has an eigenvalue equal to $\overline{\sigma_{6\kappa-3}} = -\boldsymbol{\iota}\frac{2|\mu_\kappa|\sin(\psi_\kappa^u)}{\alpha}$ (respectively, $\overline{\sigma_{6\kappa-1}} = -\boldsymbol{\iota}\frac{2|\mu_\kappa|\sin(\psi_\kappa^u)}{\alpha}$), denoted by σ_* for simplicity. In this case, Σ has exactly three zero eigenvalues, two nonzero eigenvalues are on the imaginary axis, and all other eigenvalues have negative real parts. In the following, we focus on $\theta = \theta_d^c$ because the analysis for $\theta = -\theta_d^c$ is similar except that all agents will move in reverse directions. Note from Lemma 3.1 that the right and left eigenvectors associated with $\sigma_{6\kappa-3}$ are, respectively, $\begin{bmatrix} w_\kappa\otimes\varsigma_2 \\ \sigma_{6\kappa-3}(w_\kappa\otimes\varsigma_2)\end{bmatrix}$ and $\begin{bmatrix}(\sigma_{6\kappa-3}+\alpha)(\nu_\kappa\otimes\varpi_2)\\ \nu_\kappa\otimes\varpi_2\end{bmatrix}$. We can choose $m_{6\kappa-3} = \begin{bmatrix} w_\kappa\otimes\varsigma_2 \\ \sigma_{6\kappa-3}(w_\kappa\otimes\varsigma_2)\end{bmatrix}$ and $p_{6\kappa-3} = \frac{1}{(2\sigma_{6\kappa-3}+\alpha)\nu_\kappa^T w_\kappa \varpi_2^T\varsigma_2}\begin{bmatrix}(\sigma_{6\kappa-3}+\alpha)(\nu_\kappa\otimes\varpi_2)\\ \nu_\kappa\otimes\varpi_2\end{bmatrix}$. Note that $p_{6\kappa-3}^T m_{6\kappa-3} = 1$. Similarly, it follows that m_* and p_* correspond to σ_* are given by $m_* = \overline{m_{6\kappa-3}}$ and $p_* = \overline{p_{6\kappa-3}}$. Therefore, by following a similar proof to that of the second statement of Theorem 3.2, we can show that all agents will eventually move on circular orbits with the center given by (3.7) and the period $\frac{\pi\alpha}{|\mu_\kappa\sin(\psi_\kappa^u)|}$. The radius of the orbit for agent i is given by $2|w_{\kappa(i)}p_{6\kappa-3}^T\times [r^T(0), v^T(0)]^T|\sqrt{a_2^2+a_3^2}\sin^2(\frac{\theta}{2})$. The relative radius of the orbits is equal to the relative magnitude of $w_{\kappa(i)}$. In addition, the relative phase of the agents is equal to the relative phase of $w_{\kappa(i)}$. By following a similar proof to that of the second statement of Theorem 3.2, it follows that the circular orbits are on a plane normal to the Euler axis $\mathbf{a}$.

For the fourth statement, if there exists a unique $\arg(\mu_\kappa) \in [\pi, \frac{3\pi}{2})$ such that $\psi_\kappa^u - \arg(\mu_\kappa) = \theta_d^c$ and $\theta_d^c < \theta < \min_{\arg(\mu_i)\in[\pi,\frac{3\pi}{2}),i\neq\kappa}[\psi_i^u - \arg(\mu_i)]$ (respectively, $-\min_{\arg(\mu_i)\in[\pi,\frac{3\pi}{2}),i\neq\kappa}[\psi_i^u - \arg(\mu_i)] < \theta < -\theta_d^c$), then $\lambda_{3\kappa-1} = \mu_\kappa e^{\boldsymbol{\iota}\theta} = |\mu_\kappa|e^{\boldsymbol{\iota}[\arg(\mu_\kappa)+\theta]}$ (respectively, $\lambda_{3\kappa} = \mu_\kappa e^{-\boldsymbol{\iota}\theta} = |\mu_\kappa|e^{\boldsymbol{\iota}[\arg(\mu_\kappa)-\theta]}$), where $\arg(\mu_\kappa)+\theta > \psi_\kappa^u$ (respectively, $\arg(\mu_\kappa)-\theta > \psi_\kappa^u$), which implies that $\sigma_{6\kappa-3} = \frac{-\alpha+\sqrt{\alpha^2+4\lambda_{3\kappa-1}}}{2}$ (respectively, $\sigma_{6\kappa-1} = \frac{-\alpha+\sqrt{\alpha^2+4\lambda_{3\kappa}}}{2}$) has a positive real part. A similar argument as above shows that Σ has exactly three zero eigenvalues and two eigenvalues with positive real parts and all other eigenvalues have negative real parts. By following a similar procedure to the proof of the third statement of Theorem 3.2, we can show that all agents will eventually move along logarithmic spiral curves with the center given by (3.7), the growing rate $\mathrm{Re}(\sigma_{6\kappa-3})$, and the period $\frac{2\pi}{|\mathrm{Im}(\sigma_{6\kappa-3})|}$. ■

Remark 3.6 Unlike the single-integrator case, the critical value θ_d^c for double-integrator dynamics depends on both α and $\mathcal{L}$. Note that $\theta_d^c < \theta_s^c$. When α increases to infinity, θ_d^c approaches θ_s^c. Note that besides the interaction graph and the Euler angle, α plays an important role in (3.6).

Example 3.2. To illustrate, we consider the same $\mathcal{G}$ and $\mathcal{L}$ as in Example 3.1. It can be computed that $\theta_d^c = 0.3557$ rad. Note that θ_d^c is smaller than θ_s^c in Example 3.1. Let R be the rotation matrix corresponding to the Euler axis $\mathbf{a} = \frac{1}{14}[1,2,3]^T$ and the Euler angle $\theta = \theta_d^c$. Figure 3.5 shows the eigenvalues of $-\mathcal{L}$ and $-(\mathcal{L}\otimes R)$. Note that the eigenvalues of $-(\mathcal{L}\otimes R)$ correspond to the eigenvalues of $-\mathcal{L}$ rotated by angles 0, θ, and $-\theta$. Figure 3.6 shows the eigenvalues of Σ. Note that each eigenvalue of $-(\mathcal{L}\otimes R)$, λ_k, correspond to two eigenvalues of Σ, $\sigma_{2k-1,2k}$, where $\sigma_{2k-1,2k} =$

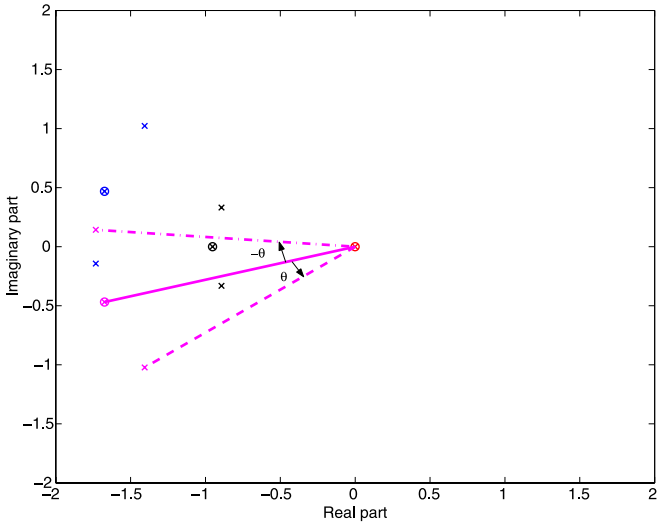

Fig. 3.5 Eigenvalues of $-\mathcal{L}$ and $-(\mathcal{L} \otimes R)$ with $\theta = \theta_d^c$. *Circles* denote the eigenvalues of $-\mathcal{L}$ while x-marks denote the eigenvalues of $-(\mathcal{L} \otimes R)$. The eigenvalues of $-(\mathcal{L} \otimes R)$ correspond to the eigenvalues of $-\mathcal{L}$ rotated by angles 0, θ, and $-\theta$, respectively. In particular, the eigenvalues obtained by rotating μ_4 by angles 0, θ, and $-\theta$ are shown by, respectively, the *solid line*, the *dashed line*, and the *dashdot line*

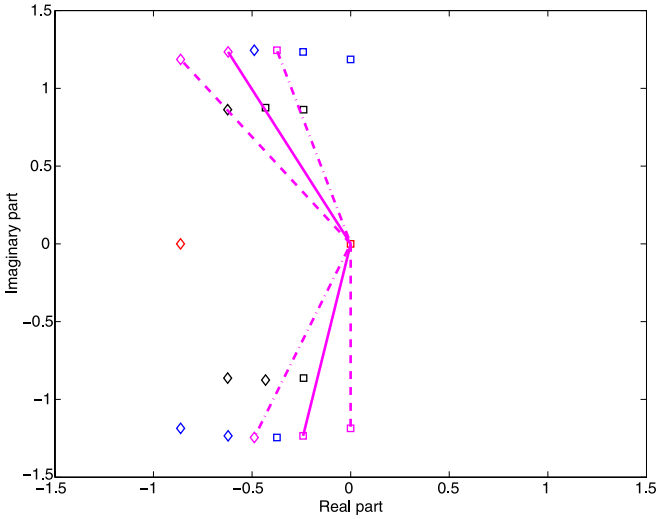

Fig. 3.6 Eigenvalues of Σ. *Squares* denote the eigenvalues computed by $\sigma_{2k-1} = \frac{-\alpha+\sqrt{\alpha^2+4\lambda_k}}{2}$ while *diamonds* denote the eigenvalues computed by $\sigma_{2k} = \frac{-\alpha-\sqrt{\alpha^2+4\lambda_k}}{2}$, $k = 1, \ldots, 12$. In particular, the eigenvalues of Σ correspond to $\lambda_{10} = \mu_4$, $\lambda_{11} = \mu_4 e^{\iota\theta}$, and $\lambda_{12} = \mu_4 e^{-\iota\theta}$ are shown by, respectively, the *solid line*, the *dashed line*, and the *dashdot line*. Because $\theta = \theta_d^c$, two nonzero eigenvalues of Σ are on the *imaginary axis*

$\frac{-\alpha\pm\sqrt{\alpha^2+4\lambda_k}}{2}$, $k = 1, \ldots, 12$. Because $\theta = \theta_d^c$, two nonzero eigenvalues of Σ are located on the imaginary axis as shown in Fig. 3.6.

3.1.3 Simulation

In this subsection, we study collective motions of four agents using, respectively, (3.2) and (3.6). Suppose that the interaction graph is given by Fig. 3.1 and $\mathcal{L}$ is given by (3.4). Let θ_s^c, θ_d^c, and $\mathbf{a}$ be given in Examples 3.1 and 3.2. Using (3.6), it can be computed that $\alpha^c = 0.3626$. We let $\alpha = 0.8626$. Note that there exists a unique $\arg(\mu_4) \in [\pi, \frac{3\pi}{2})$ such that $\psi_4^u - \arg(\mu_4) = \theta_d^c$ (i.e., $\kappa = 4$ in Theorem 3.5). Note that a right eigenvector of $-\mathcal{L}$ associated with the eigenvalue μ_4 is $w_4 = [-0.2847 - 0.2820\boldsymbol{\imath}, 0.7213, -0.2501 + 0.1355\boldsymbol{\imath}, 0.4809 + 0.0837\boldsymbol{\imath}]^T$. Also note that $\mathbf{p} = [0.2502, 0.1911, 0.4587, 0.1001]^T$.

Figures 3.7, 3.8, and 3.9 show, respectively, the trajectories of the four agents using (3.2) with $\theta = \frac{\theta_s^c}{2}$, $\theta = \theta_s^c$, and $\theta_s^c + 0.1$. Note that all agents eventually rendezvous when $\theta = \frac{\theta_s^c}{2}$, move on circular orbits when $\theta = \theta_s^c$, and move along logarithmic spiral curves when $\theta = \theta_s^c + 0.1$. Also note that when $\theta = \theta_s^c$, the relative radius of the circular orbits (respectively, the relative phase of the agents) is equal to the relative magnitude (respectively, phase) of the components of w_4. In addition, the trajectories of all agents are normal to the Euler axis $\mathbf{a}$ in all cases.

Figures 3.10, 3.11, 3.12, and 3.13 show, respectively, the trajectories of the four agents using (3.6) with $R = I_3$, $\theta = \theta_d^c - 0.2$, $\theta = \theta_d^c$, and $\theta = \theta_d^c + 0.2$. Note that all agents eventually rendezvous at the position given by (3.7) when $R = I_3$ or

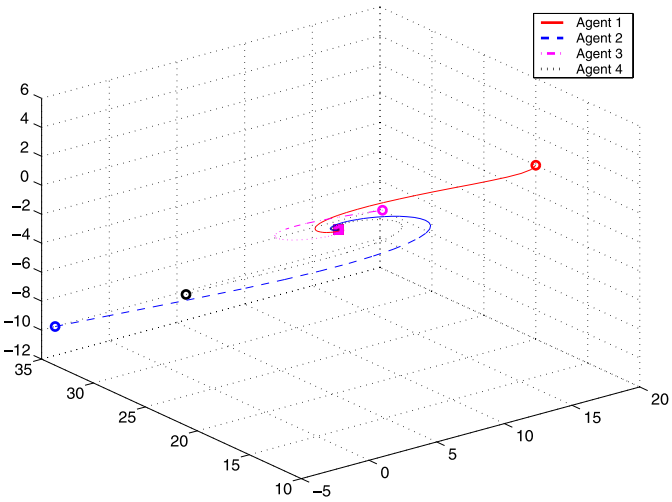

Fig. 3.7 Trajectories of the four agents using (3.2) with $\theta = \frac{\theta_s^c}{2}$. *Circles* denote the starting positions of the agents while the *squares* denote the snapshots of the agents at 10 s

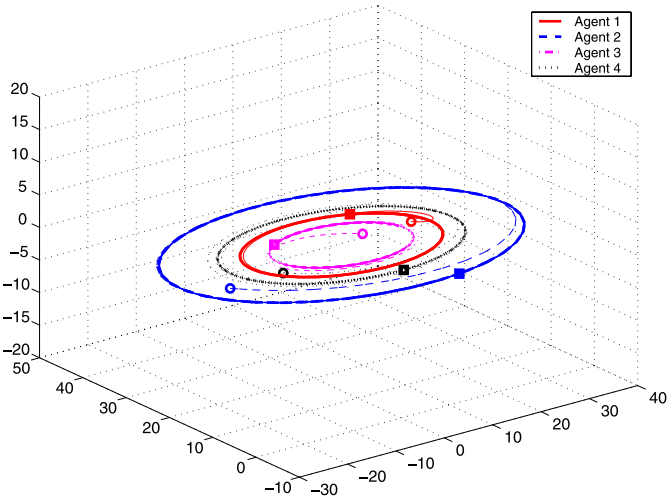

Fig. 3.8 Trajectories of the four agents using (3.2) with $\theta = \theta_s^c$. *Circles* denote the starting positions of the agents while the *squares* denote the snapshots of the agents at 30 s

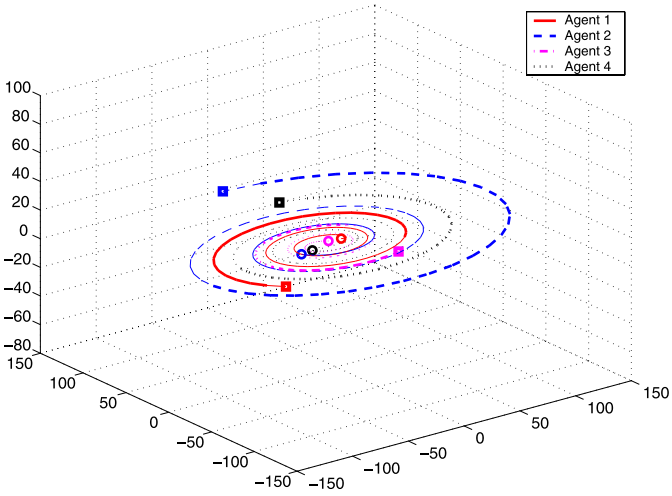

Fig. 3.9 Trajectories of the four agents using (3.2) with $\theta = \theta_s^c + 0.1$. *Circles* denote the starting positions of the agents while the *squares* denote the snapshots of the agents at 10 s

$\theta = \theta_d^c - 0.2$, move on circular orbits when $\theta = \theta_d^c$, and move along logarithmic spiral curves when $\theta = \theta_d^c + 0.2$. While similar motions to those using (3.2) are observed, the critical value for the Euler angle, the period of the circular motion, and the period and the growing rate of the logarithmic spiral motion using (3.6) are different from those using (3.2) even if the interaction graph and $\mathcal{L}$ are chosen to be the same.

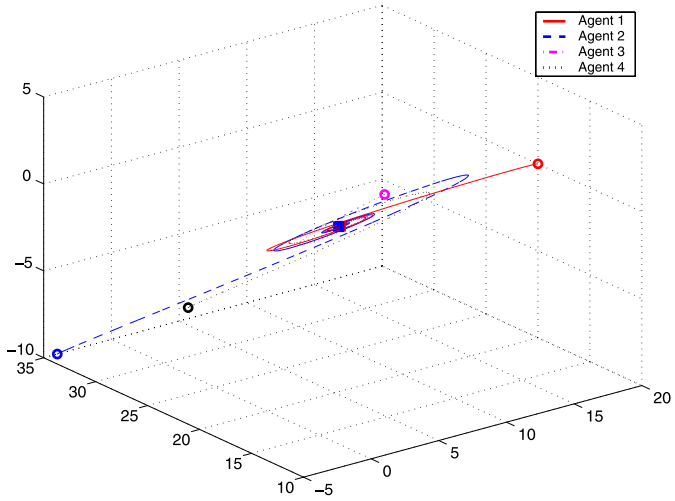

Fig. 3.10 Trajectories of the four agents using (3.6) with $R = I_3$. *Circles* denote the starting positions of the agents while the *squares* denote the snapshots of the agents at 20 s

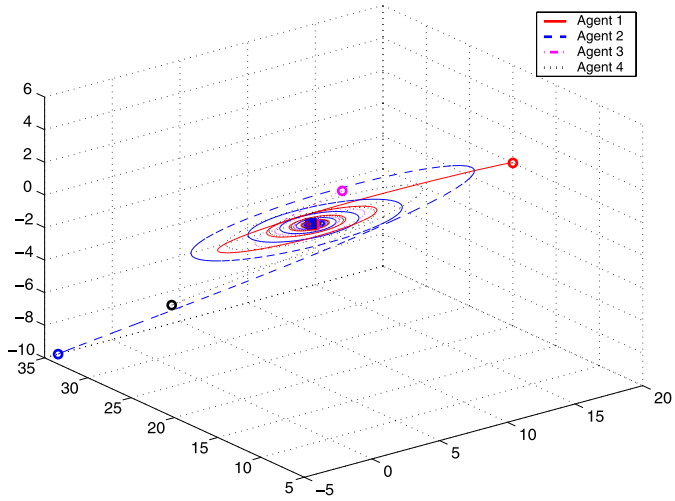

Fig. 3.11 Trajectories of the four agents using (3.6) with $\theta = \theta_d^c - 0.2$. *Circles* denote the starting positions of the agents while the *squares* denote the snapshots of the agents at 30 s

3.2 Coupled Harmonic Oscillators

In this section, we study coupled second-order linear harmonic oscillators with local interaction to achieve synchronized oscillatory motions. We will analyze convergence conditions under, respectively, directed fixed and switching interaction graphs.

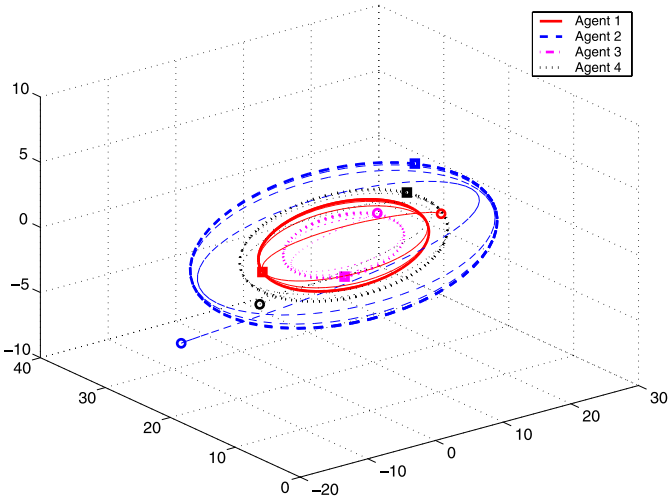

Fig. 3.12 Trajectories of the four agents using (3.6) with $\theta = \theta_d^c$. *Circles* denote the starting positions of the agents while the *squares* denote the snapshots of the agents at 30 s

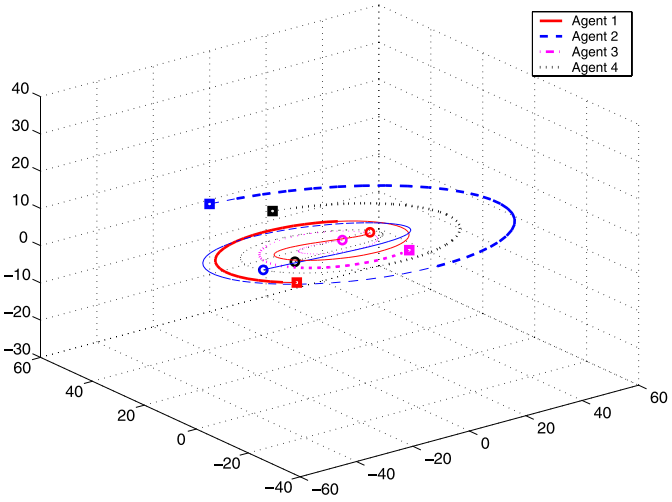

Fig. 3.13 Trajectories of the four agents using (3.6) with $\theta = \theta_d^c + 0.2$. *Circles* denote the starting positions of the agents while the *squares* denote the snapshots of the agents at 10 s

3.2.1 Problem Statement

When two objects of mass m are connected by a damper with the coefficient b and are each attached to fixed supports by identical springs with the spring constant k,

they can be represented by

$$m\ddot{x}_1 + kx_1 + b(\dot{x}_1 - \dot{x}_2) = 0, \tag{3.10a}$$
$$m\ddot{x}_2 + kx_2 + b(\dot{x}_2 - \dot{x}_1) = 0, \tag{3.10b}$$

where $x_i \in \mathbb{R}$ denotes the position of the ith object. Motivated by (3.10), we study n coupled harmonic oscillators with local interaction of the form

$$\ddot{x}_i + \alpha(t)x_i + \sum_{j=1}^{n} a_{ij}(t)(\dot{x}_i - \dot{x}_j) = 0, \quad i = 1, \ldots, n, \tag{3.11}$$

where $x_i \in \mathbb{R}$ is the position of the ith oscillator, $\alpha(t)$ is a positive gain at time t, and $a_{ij}(t)$ is the (i, j)th entry of the adjacency matrix $\mathcal{A}(t)$ associated with the directed graph $\mathcal{G}(t) \triangleq [\mathcal{V}, \mathcal{E}(t)]$ characterizing the interaction among the n oscillators at time t (i.e., $a_{ij}(t) > 0$ if oscillator i can obtain the velocity of oscillator j at time t and $a_{ij}(t) = 0$ otherwise). While (3.11) conceptually represents a system where n virtual masses are connected by virtual dampers, the purpose of this section is to adopt (3.11) as a distributed algorithm for synchronization of the positions and velocities of n networked point-mass agents.

Let $r_i \triangleq x_i$ and $v_i \triangleq \dot{x}_i$. Equation (3.11) can be written as

$$\dot{r}_i = v_i,$$
$$\dot{v}_i = -\alpha(t)r_i - \sum_{j=1}^{n} a_{ij}(t)(v_i - v_j), \quad i = 1, \ldots, n. \tag{3.12}$$

Let $r \triangleq [r_1, \ldots, r_n]^T$ and $v \triangleq [v_1, \ldots, v_n]^T$. Equation (3.12) can be written in a vector form as

$$\begin{bmatrix} \dot{r} \\ \dot{v} \end{bmatrix} = \underbrace{\begin{bmatrix} 0_{n\times n} & I_n \\ -\alpha(t)I_n & -\mathcal{L}(t) \end{bmatrix}}_{\mathcal{Q}} \begin{bmatrix} r \\ v \end{bmatrix}, \tag{3.13}$$

where $\mathcal{L}(t) \in \mathbb{R}^{n\times n}$ is the nonsymmetric Laplacian matrix associated with $\mathcal{A}(t)$ and hence $\mathcal{G}(t)$ at time t. In the following, we focus on the one-dimensional space for simplicity of presentation. However, all results hereafter are still valid for any high-dimensional space by use of the properties of the Kronecker product.

3.2.2 *Convergence Under Directed Fixed Interaction*

In this subsection, we consider convergence of (3.12) under a directed fixed interaction graph. Here we assume that both α and $\mathcal{L}$ in (3.13) are constant. Both leaderless and leader-following cases will be addressed. We need the following lemmas for our main result.

Lemma 3.2. *Let μ_i be the ith eigenvalue of $-\mathcal{L}$. Also let $\chi_{ri} \in \mathbb{C}^n$ and $\chi_{\ell i} \in \mathbb{C}^n$ be, respectively, the right and left eigenvectors of $-\mathcal{L}$ associated with μ_i. Then the eigenvalues of $\mathcal{Q}$, defined in (3.13), are given by $\lambda_{i\pm} = \frac{\mu_i \pm \sqrt{\mu_i^2 - 4\alpha}}{2}$ with the associated right eigenvectors $\varphi_{ri\pm} = [\chi_i^T, \lambda_{i\pm}\chi_i^T]^T$ and left eigenvectors $\varphi_{\ell i\pm} = [\chi_{\ell i}^T, -\frac{\lambda_{i\pm}}{\alpha}\chi_{\ell i}^T]^T$.*

Proof: Let λ be an eigenvalue of $\mathcal{Q}$ and $\varphi_r = [x_r^T, y_r^T]^T \in \mathbb{C}^{2n}$ be an associated right eigenvector. Then we get that

$$\begin{bmatrix} 0_{n\times n} & I_n \\ -\alpha I_n & -\mathcal{L} \end{bmatrix} \begin{bmatrix} x_r \\ y_r \end{bmatrix} = \lambda \begin{bmatrix} x_r \\ y_r \end{bmatrix}. \tag{3.14}$$

It follows from (3.14) that

$$y_r = \lambda x_r, \tag{3.15a}$$
$$-\alpha x_r - \mathcal{L} y_r = \lambda y_r. \tag{3.15b}$$

Combining (3.15a) and (3.15b) gives $-\mathcal{L}x_r = \frac{\lambda^2+\alpha}{\lambda}x_r$. Suppose that μ is an eigenvalue of $-\mathcal{L}$ with an associated right eigenvector χ_r. It follows that $\frac{\lambda^2+\alpha}{\lambda} = \mu$ and $x_r = \chi_r$. Therefore, it follows that λ satisfies

$$\lambda^2 - \mu\lambda + \alpha = 0 \tag{3.16}$$

and $\varphi_r = [\chi_r^T, \lambda\chi_r^T]^T$ according to (3.15a). Noting that μ_i is the ith eigenvalue of $-\mathcal{L}$ with an associated right eigenvector χ_{ri}, it follows from (3.16) that the eigenvalues of $\mathcal{Q}$ are given by $\lambda_{i\pm} = \frac{\mu_i \pm \sqrt{\mu_i^2 - 4\alpha}}{2}$ with the associated right eigenvectors $\varphi_{ri\pm} = [\chi_{ri}^T, \lambda_{i\pm}\chi_{ri}^T]^T$.

Similarly, let $\varphi_\ell = [x_\ell^T, y_\ell^T]^T \in \mathbb{C}^{2n}$ be a left eigenvector of $\mathcal{Q}$ associated with the eigenvalue λ. Then we get that

$$[x_\ell^T, y_\ell^T] \begin{bmatrix} 0_{n\times n} & I_n \\ -\alpha I_n & -\mathcal{L} \end{bmatrix} = \lambda [x_\ell^T, y_\ell^T]. \tag{3.17}$$

It follows from (3.17) that

$$y_\ell^T = -\frac{\lambda}{\alpha} x_\ell^T, \tag{3.18a}$$
$$x_\ell^T - y_\ell^T \mathcal{L} = \lambda y_\ell^T. \tag{3.18b}$$

Combining (3.18a) and (3.18b) gives that $-x_\ell^T\mathcal{L} = \frac{\lambda^2+\alpha}{\lambda}x_\ell^T$. A similar argument to that of the right eigenvectors shows that the left eigenvectors of $\mathcal{Q}$ associated with $\lambda_{i\pm}$ are $\varphi_{\ell i\pm} = [\chi_{\ell i}^T, -\frac{\lambda_{i\pm}}{\alpha}\chi_{\ell i}^T]^T$. ■

In the leaderless case, we have the following theorem.

Theorem 3.7. *Let $\mathbf{p} \in \mathbb{R}^n$ be defined in Lemma 1.1. Let μ_i, $\lambda_{i\pm}$, $\varphi_{ri\pm}$, and $\varphi_{\ell i\pm}$ be defined in Lemma 3.2. Suppose that the directed graph $\mathcal{G}$ has a directed spanning*

tree. Using (3.12), $|r_i(t) - [\cos(\sqrt{\alpha}t)\mathbf{p}^T r(0) + \frac{1}{\sqrt{\alpha}}\sin(\sqrt{\alpha}t)\mathbf{p}^T v(0)]| \to 0$ *and* $|v_i(t) - [-\sqrt{\alpha}\sin(\sqrt{\alpha}t)\mathbf{p}^T r(0) + \cos(\sqrt{\alpha}t)\mathbf{p}^T v(0)]| \to 0$ *as* $t \to \infty$.

Proof: Note that the directed graph $\mathcal{G}$ has a directed spanning tree. It follows from Lemma 1.1 that $-\mathcal{L}$ has a simple zero eigenvalue with an associated right eigenvector $\mathbf{1}_n$ and left eigenvector $\mathbf{p}$ that satisfies $\mathbf{p} \geq 0$, $\mathbf{p}^T\mathcal{L} = 0$, and $\mathbf{p}^T\mathbf{1}_n = 1$. In addition, all other eigenvalues of $-\mathcal{L}$ have negative real parts. Without loss of generality, let $\mu_1 = 0$ and then we get that $\mathrm{Re}(\mu_i) < 0$, $i = 2, \ldots, n$. Accordingly, it follows from Lemma 3.2 that $\lambda_{1\pm} = \pm\sqrt{\alpha}\boldsymbol{\imath}$ with the associated right and left eigenvectors given by

$$\varphi_{r1\pm} = \left[\mathbf{1}_n^T, \pm\sqrt{\alpha}\boldsymbol{\imath}\mathbf{1}_n^T\right]^T, \qquad \varphi_{\ell 1\pm} = \left[\mathbf{p}^T, \pm\frac{1}{\sqrt{\alpha}\boldsymbol{\imath}}\mathbf{p}^T\right]^T. \tag{3.19}$$

Because $\mathrm{Re}(\mu_i) < 0$, $i = 2, \ldots, n$, it follows that $\mathrm{Re}(\lambda_{i-}) = \mathrm{Re}(\frac{\mu_i - \sqrt{\mu_i^2 - 4\alpha}}{2}) < 0$, $i = 2, \ldots, n$. Noting that $\lambda_{i+}\lambda_{i-} = \alpha$, $i = 2, \ldots, n$, it follows that $\arg(\lambda_{i+}) = -\arg(\lambda_{i-})$. Therefore, it follows that $\mathrm{Re}(\lambda_{i+}) < 0$, $i = 2, \ldots, n$.

Note that $\mathcal{Q}$ can be written in the Jordan canonical form as

$$\mathcal{Q} = \underbrace{[w_1, \ldots, w_{2n}]}_{P} \begin{bmatrix} \sqrt{\alpha}\boldsymbol{\imath} & 0 & 0_{1\times(2n-2)} \\ 0 & -\sqrt{\alpha}\boldsymbol{\imath} & 0_{1\times(2n-2)} \\ 0_{(2n-2)\times 1} & 0_{(2n-2)\times 1} & \overline{J} \end{bmatrix} \underbrace{\begin{bmatrix} \nu_1^T \\ \vdots \\ \nu_{2n}^T \end{bmatrix}}_{P^{-1}}, \tag{3.20}$$

where $w_i \in \mathbb{R}^{2n}$, $i = 1, \ldots, 2n$, can be chosen to be the right eigenvectors or generalized eigenvectors of $\mathcal{Q}$, $\nu_i \in \mathbb{R}^{2n}$, $i = 1, \ldots, 2n$, can be chosen to be the left eigenvectors or generalized eigenvectors of $\mathcal{Q}$, and $\overline{J}$ is the Jordan upper diagonal block matrix corresponding to the eigenvalues λ_{i+} and λ_{i-}, $i = 2, \ldots, n$. Because $P^{-1}P = I_{2n}$, w_i and ν_i must satisfy that $\nu_i^T w_i = 1$ and $\nu_i^T w_k = 0$, where $i \neq k$. Accordingly, we let $w_1 = \varphi_{r1+}$, $w_2 = \varphi_{r1-}$, $\nu_1 = \frac{1}{2}\varphi_{\ell 1+}$, and $\nu_2 = \frac{1}{2}\varphi_{\ell 1-}$, where $\varphi_{r1\pm}$ and $\varphi_{\ell\pm}$ are defined in (3.19).

Let

$$\begin{aligned} \Phi(t) &\triangleq e^{\sqrt{\alpha}\boldsymbol{\imath}t}\begin{bmatrix}\mathbf{1}_n \\ \sqrt{\alpha}\boldsymbol{\imath}\mathbf{1}_n\end{bmatrix}\left[\frac{1}{2}\mathbf{p}^T, \frac{1}{2\sqrt{\alpha}\boldsymbol{\imath}}\mathbf{p}^T\right] \\ &\quad + e^{-\sqrt{\alpha}\boldsymbol{\imath}t}\begin{bmatrix}\mathbf{1}_n \\ -\sqrt{\alpha}\boldsymbol{\imath}\mathbf{1}_n\end{bmatrix}\left[\frac{1}{2}\mathbf{p}^T, -\frac{1}{2\sqrt{\alpha}\boldsymbol{\imath}}\mathbf{p}^T\right] \\ &= \begin{bmatrix}\cos(\sqrt{\alpha}t)\mathbf{1}_n\mathbf{p}^T & \frac{1}{\sqrt{\alpha}}\sin(\sqrt{\alpha}t)\mathbf{1}_n\mathbf{p}^T \\ -\sqrt{\alpha}\sin(\sqrt{\alpha}t)\mathbf{1}_n\mathbf{p}^T & \cos(\sqrt{\alpha}t)\mathbf{1}_n\mathbf{p}^T\end{bmatrix}. \end{aligned}$$

Because $e^{\mathcal{Q}t} = Pe^{Jt}P^{-1}$ and $\lim_{t\to\infty} e^{\overline{J}t} = 0_{(2n-2)\times(2n-2)}$, it follows that $\lim_{t\to\infty}\|e^{\mathcal{Q}t} - \Phi(t)\| = 0$. The solution to (3.13) is given by $\left[\begin{smallmatrix} r(t) \\ v(t)\end{smallmatrix}\right] = e^{\mathcal{Q}t}\left[\begin{smallmatrix} r(0) \\ v(0)\end{smallmatrix}\right]$.

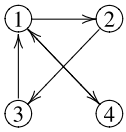

Fig. 3.14 Directed fixed graph $\mathcal{G}$. An *arrow* from j to i denotes that agent j is a neighbor of agent i

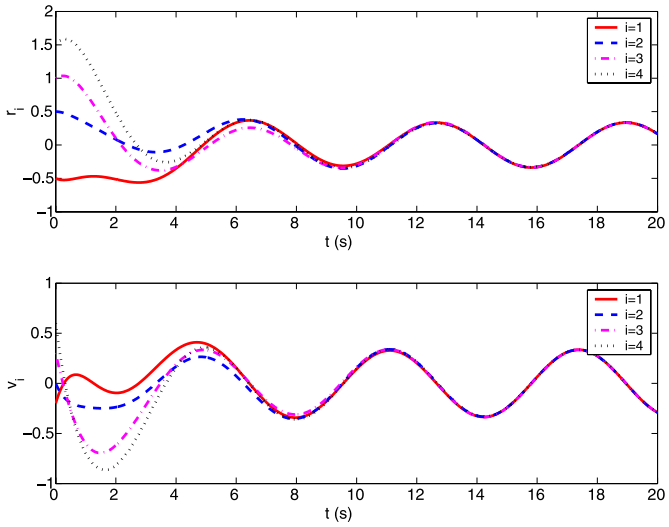

Fig. 3.15 Evolution of the oscillator states using (3.12) with $\alpha = 1$ and $\mathcal{G}$ shown in Fig. 3.14

Therefore, it follows that

$$\left| r_i(t) - \left[\cos\left(\sqrt{\alpha}t\right)\mathbf{p}^T r(0) + \frac{1}{\sqrt{\alpha}} \sin\left(\sqrt{\alpha}t\right)\mathbf{p}^T v(0) \right] \right| \to 0$$

and

$$\left| v_i(t) - \left[-\sqrt{\alpha} \sin\left(\sqrt{\alpha}t\right)\mathbf{p}^T r(0) + \cos\left(\sqrt{\alpha}t\right)\mathbf{p}^T v(0) \right] \right| \to 0$$

as $t \to \infty$. ■

Example 3.3. To illustrate, we show simulation results involving four coupled harmonic oscillators using (3.12) under the directed fixed graph $\mathcal{G}$ as shown in Fig. 3.14. Note that $\mathcal{G}$ in this case has a directed spanning tree, implying that the condition of Theorem 3.7 is satisfied. We assume that $a_{ij} = 1$ if $(j, i) \in \mathcal{E}$ and $a_{ij} = 0$ otherwise. Figures 3.15 and 3.16 show, respectively, the evolution of the oscillator states with $\alpha = 1$ and $\alpha = 4$. Note that the oscillator states are synchronized for both $\alpha = 1$ and $\alpha = 4$. However, the value of α has an effect on the amplitude and frequency of the synchronized states.

Under the condition of Theorem 3.7, all r_i converge to a common oscillatory trajectory, so do all v_i. That is, the n coupled harmonic oscillators are synchronized.

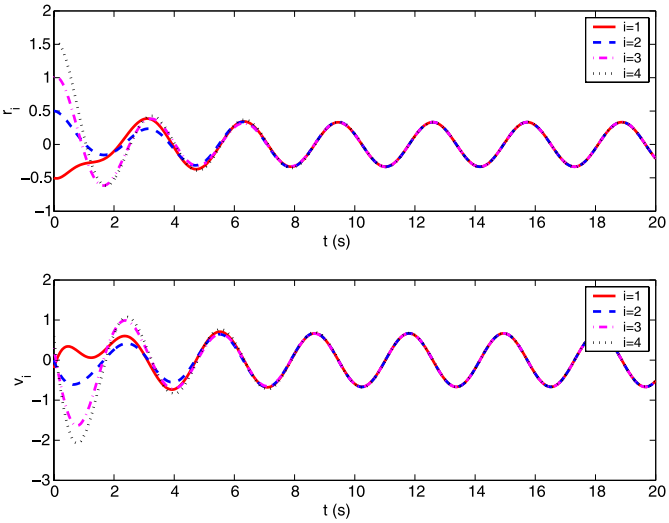

Fig. 3.16 Evolution of the oscillator states using (3.12) with $\alpha = 4$ and $\mathcal{G}$ shown in Fig. 3.14

We next consider the case where there exist n followers, labeled as oscillators or followers 1 to n, and a leader, labeled as oscillator 0 with states r_0 and v_0. Here the leader can be virtual or physical. Let $\mathcal{G} \triangleq (\mathcal{V}, \mathcal{E})$ be the directed graph characterizing the interaction among the n followers. Let $\overline{\mathcal{G}} \triangleq (\overline{\mathcal{V}}, \overline{\mathcal{E}})$ be the directed graph characterizing the interaction among the leader and the followers corresponding to $\mathcal{G}$.

Suppose that r_0 and v_0 satisfy

$$\dot{r}_0 = v_0, \qquad \dot{v}_0 = -\alpha r_0, \tag{3.21}$$

where α is a positive gain. In this case, we study the system

$$\begin{aligned} \dot{r}_i &= v_i, \\ \dot{v}_i &= -\alpha r_i - \sum_{j=0}^{n} a_{ij}(v_i - v_j), \quad i = 1, \ldots, n, \end{aligned} \tag{3.22}$$

where $a_{ij}, i, j = 1, \ldots, n$ is the (i, j)th entry of the adjacency matrix $\mathcal{A}$ associated with $\mathcal{G}$, and a_{i0} is a positive constant if the leader is a neighbor of oscillator i and $a_{i0} = 0$ otherwise.

Corollary 3.3. *Suppose that in $\overline{\mathcal{G}}$ the leader has directed paths to all followers* 1 *to* n. *Using* (3.22), $|r_i(t) - r_0(t)| \to 0$ *and* $|v_i(t) - v_0(t)| \to 0$ *as* $t \to \infty$, *where*

$$\begin{aligned} r_0(t) &= \cos\big(\sqrt{\alpha}t\big) r_0(0) + \frac{1}{\alpha} \sin\big(\sqrt{\alpha}t\big) v_0(0), \\ v_0(t) &= -\sqrt{\alpha} \sin\big(\sqrt{\alpha}t\big) r_0(0) + \cos\big(\sqrt{\alpha}t\big) v_0(0). \end{aligned} \tag{3.23}$$

Proof: It is straightforward to show that the solution to (3.21) is given by (3.23). Consider a team consisting of $n+1$ oscillators (oscillators 0 to n). The proof is a direct application of that of Theorem 3.7. ■

We also consider the case where there exist deviations between oscillator states. In this case, we study the system

$$\begin{aligned} \dot{r}_i &= v_i, \\ \dot{v}_i &= -\alpha(r_i - \delta_i) - \sum_{j=0}^{n} a_{ij}(v_i - v_j), \quad i = 1, \ldots, n, \end{aligned} \tag{3.24}$$

where δ_i is a constant, and α and $a_{ij}, i = 1, \ldots, n, j = 0, \ldots, n$ are defined as in (3.22).

Corollary 3.4. *Suppose that in $\overline{\mathcal{G}}$ the leader has directed paths to all followers 1 to n. Using (3.24), $|r_i(t) - [r_0(t) + \delta_i]| \to 0$ and $|v_i(t) - v_0(t)| \to 0$ as $t \to \infty$, where $r_0(t)$ and $v_0(t)$ are defined in Corollary 3.3.*

Proof: Let $\tilde{r}_i \triangleq r_i - \delta_i$. Noting that $\dot{\tilde{r}}_i = v_i$, it follows from Corollary 3.3 that $|\tilde{r}_i(t) - r_0(t)| \to 0$ and $|v_i(t) - v_0(t)| \to 0$ as $t \to \infty$ with $\tilde{r}_i$ playing the role of r_i in (3.22). ■

3.2.3 Convergence Under Directed Switching Interaction

In this subsection, we consider convergence of (3.12) under a directed switching interaction graph. We consider two cases, namely, (i) the directed graph $\mathcal{G}(t)$ is strongly connected and balanced at each time instant; and (ii) the directed graph $\mathcal{G}(t)$ has a directed spanning tree at each time instant.

Let $\mathcal{P}$ denote a set indexing the class of all possible directed graphs $\mathcal{G}_p$, where $p \in \mathcal{P}$, defined on n nodes. The adjacency matrix and the nonsymmetric Laplacian matrix associated with $\mathcal{G}_p$ are denoted by, respectively, $\mathcal{A}_p$ and $\mathcal{L}_p$. Note that $\mathcal{P}$ is a finite set by definition. Suppose that (3.12) can be written as

$$\begin{bmatrix} \dot{r} \\ \dot{v} \end{bmatrix} = \underbrace{\begin{bmatrix} 0_{n\times n} & I_n \\ -\alpha_{\sigma(t)} I_n & -\mathcal{L}_{\sigma(t)} \end{bmatrix}}_{\mathcal{Q}_{\sigma(t)}} \begin{bmatrix} r \\ v \end{bmatrix}, \tag{3.25}$$

where $\sigma : [0, \infty) \mapsto \mathcal{P}$ is a piecewise constant switching signal with switching times $t_0, t_1, \ldots$, $\alpha_{\sigma(t)}$ is a positive gain associated with the directed graph $\mathcal{G}_{\sigma(t)}$, and $\mathcal{L}_{\sigma(t)}$ is the nonsymmetric Laplacian matrix associated with $\mathcal{A}_{\sigma(t)}$ and hence $\mathcal{G}_{\sigma(t)}$.

Theorem 3.8. *Suppose that $\sigma(t) \in \mathcal{P}_{sb}$, where $\mathcal{P}_{sb} \subset \mathcal{P}$ denotes the set indexing the class of all possible directed graphs defined on n nodes that are strongly connected and balanced. Also suppose that $\alpha_{\sigma(t)} \equiv \alpha_{sb}$, where α_{sb} is a positive scalar. Using (3.12), $|r_i(t) - r_j(t)| \to 0$ and $|v_i(t) - v_j(t)| \to 0$ as $t \to \infty$.*

Proof: [5] Consider the Lyapunov function candidate

$$V = \frac{1}{2}\alpha_{sb} r^T r + \frac{1}{2} v^T v. \tag{3.26}$$

Noting that $\dot{v}$ is discontinuous due to switches of interaction graphs, we have $\dot{v} \in^{a.e.} K[-\mathcal{L}_{\sigma(t)} v] - \alpha_{sb} r$, where $K[\cdot]$ is a differential inclusion and $a.e.$ stands for "almost everywhere". The set-valued Lie derivative of V is given by $\widetilde{L}_F V = \alpha_{sb} v^T r + v^T[-\alpha_{sb} r + \phi_v] = v^T \phi_v$, where ϕ_v is an arbitrary element of $K[-\mathcal{L}_{\sigma(t)} v]$. Note that the directed graph $\mathcal{G}_{\sigma(t)}$ is strongly connected and balanced. It follows from Lemma 1.2 that $-v^T \mathcal{L}_{\sigma(t)} v \leq 0$, which implies that $\max_{\phi_v \in K[-\mathcal{L}_{\sigma(t)} v]}(v^T \phi_v) = \max(K[-v^T \mathcal{L}_{\sigma(t)} v]) = 0$. In particular, $\max(K[-v^T \mathcal{L}_{\sigma(t)} v]) = 0$ if and only if $v_i = v_j$, which in turn implies that $\dot{v}_i = \dot{v}_j$. Noting that $\alpha_{\sigma(t)} \equiv \alpha_{sb}$, it follows from (3.25) (see also (3.12)) that $r_i = r_j$ when $v_i = v_j$ and $\dot{v}_i = \dot{v}_j$. It thus follows from Lemma 1.40 that $|r_i(t) - r_j(t)| \to 0$ and $|v_i(t) - v_j(t)| \to 0$ as $t \to \infty$. ■

Let $r_{ij} \triangleq r_i - r_j$ and $v_{ij} \triangleq v_i - v_j$. Also let $\tilde{r} \triangleq [r_{12}, r_{23}, \ldots, r_{(n-1)n}]^T$ and $\tilde{v} \triangleq [v_{12}, v_{23}, \ldots, v_{(n-1)n}]^T$. Equation (3.25) can be rewritten as

$$\begin{bmatrix} \dot{\tilde{r}} \\ \dot{\tilde{v}} \end{bmatrix} = \underbrace{\begin{bmatrix} 0_{n-1} & I_{n-1} \\ -\alpha_{\sigma(t)} I_{n-1} & -\mathcal{D}_{\sigma(t)} \end{bmatrix}}_{\mathcal{R}_{\sigma(t)}} \begin{bmatrix} \tilde{r} \\ \tilde{v} \end{bmatrix}, \tag{3.27}$$

where $\mathcal{D}_{\sigma(t)} \in \mathbb{R}^{(n-1)\times(n-1)}$ can be derived from $\mathcal{L}_{\sigma(t)}$. Before moving on, we need the following lemma.

Lemma 3.3 ([201, Lemma 2]). *Let $\{A_p : p \in \mathcal{P}\}$ be a closed bounded set of real $n \times n$ matrices. Suppose that for each $p \in \mathcal{P}$, A_p is stable, and let a_p and χ_p be any finite nonnegative and positive numbers, respectively, for which $\|e^{A_p t}\| \leq e^{a_p - \chi_p t}$, $t \geq 0$. Suppose that τ_0 is a number satisfying $\tau_0 > \sup_{p\in\mathcal{P}}\{\frac{a_p}{\chi_p}\}$. For any admissible switching signal $\sigma : [0, \infty) \to \mathcal{P}$ with dwell time no smaller than τ_0, the transition matrix of A_σ satisfies that $\|\Phi(t, \mu)\| \leq e^{a - \chi(t-\mu)}$, $\forall t \geq \mu \geq 0$, where $a \triangleq \sup_{p\in\mathcal{P}}\{a_p\}$ and $\chi \triangleq \inf_{p\in\mathcal{P}}\{\chi_p - \frac{a_p}{\tau_0}\}$.*

Theorem 3.9. *Let $\mathcal{P}_{st} \subset \mathcal{P}$ denote the set indexing the class of all possible directed graphs defined on n nodes that have a directed spanning tree. The following two statements hold*:

1. *The matrix $\mathcal{R}_p$ defined in (3.27) is stable for each $p \in \mathcal{P}_{st}$.*
2. *Let $a_p \geq 0$ and $\chi_p > 0$, for which $\|e^{\mathcal{R}_p t}\| \leq e^{a_p - \chi_p t}$, $t \geq 0$. Suppose that $\sigma(t) \in \mathcal{P}_{st}$. If $t_{k+1} - t_k > \sup_{p\in\mathcal{P}_{st}}\{\frac{a_p}{\chi_p}\}$, $\forall k = 0, 1, \ldots$, then using (3.12), $|r_i(t) - r_j(t)| \to 0$ and $|v_i(t) - v_j(t)| \to 0$ as $t \to \infty$.*

[5] The proof is motivated by that of Theorem 1 in [289], which relies on differential inclusions and nonsmooth analysis. We only sketch the main steps of the proof.

Proof: For the first statement, note that Theorem 3.7 implies that for each $p \in \mathcal{P}_{st}$ and all $i, j = 1, \ldots, n$, $|r_i(t) - r_j(t)| \to 0$ and $|v_i(t) - v_j(t)| \to 0$ as $t \to \infty$, which implies that $\|\tilde{r}(t)\| \to 0$ and $\|\tilde{v}(t)\| \to 0$ as $t \to \infty$. It thus follows from (3.27) that $\mathcal{R}_p$ is stable for each $p \in \mathcal{P}_{st}$.

For the second statement, under the condition of the theorem, because $\mathcal{R}_p$ is stable for each $p \in \mathcal{P}_{st}$, it follows from Lemma 3.3 that the switched system (3.27) is globally exponentially stable if $t_{k+1} - t_k > \sup_{p \in \mathcal{P}_{st}} \{\frac{\alpha_p}{\chi_p}\}$, $\forall k = 0, 1, \ldots$. Equivalently, it follows that under the same condition $|r_i(t) - r_j(t)| \to 0$ and $|v_i(t) - v_j(t)| \to 0$ as $t \to \infty$. ■

Remark 3.10 Note that Theorem 3.9 imposes a bound on how fast the interaction graph can switch while Theorem 3.8 does not. Also note that the convergence condition in Theorem 3.9 is only a sufficient condition. When there exists a leader, the analysis can follow a similar line to that of Theorems 3.8 and 3.9.

Example 3.4. To illustrate, we show simulation results involving four coupled harmonic oscillators using (3.12) under a directed switching interaction graph. We first let $\alpha_{\sigma(t)} \equiv 1$ and $\mathcal{G}(t)$ switches randomly from $\{\mathcal{G}_{(1)}, \mathcal{G}_{(2)}, \mathcal{G}_{(3)}\}$ as shown in Fig. 3.17. We assume that $a_{ij} = 1$ if $(j, i) \in \mathcal{E}$ and $a_{ij} = 0$ otherwise. Here we let $t_0 = 0$ s and choose t_k randomly from $(2k - 2, 2k)$ s, $k = 1, 2, \ldots$. Note that $\mathcal{G}_{(1)}$–$\mathcal{G}_{(3)}$ shown in Fig. 3.17 are all strongly connected and balanced, implying that the condition of Theorem 3.8 is satisfied. Figure 3.18 shows the evolution of the oscillator states in this case. Note that all oscillator states are synchronized. We then let $\alpha_{\sigma(t)}$ switch randomly from $\{\alpha_{(1)}, \alpha_{(2)}, \alpha_{(3)}\}$, where

$$\alpha_{(1)} = 1, \qquad \alpha_{(2)} = 4, \qquad \alpha_{(3)} = 9 \tag{3.28}$$

and $\mathcal{G}(t)$ switches randomly from $\{\mathcal{G}_{(1)}, \mathcal{G}_{(2)}, \mathcal{G}_{(3)}\}$ as shown in Fig. 3.19. Here we again let $t_0 = 0$ s and choose t_k randomly from $(2k - 2, 2k)$ s, $k = 1, 2, \ldots$. Note that $\mathcal{G}_{(1)}$–$\mathcal{G}_{(3)}$ shown in Fig. 3.19 all have a directed spanning tree, implying that the condition of Theorem 3.9 is satisfied. Figure 3.20 shows the evolution of the oscillator states in this case. In contrast to the previous case, the oscillator states do not approach a uniform amplitude and frequency due to switching of α values. However, all oscillator states are still synchronized.

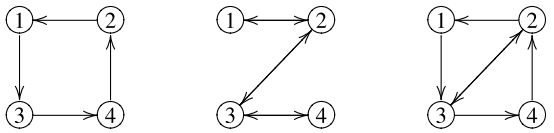

(a) $\mathcal{G}_{(1)}$ (b) $\mathcal{G}_{(2)}$ (c) $\mathcal{G}_{(3)}$

Fig. 3.17 Directed graphs $\mathcal{G}_{(1)}$–$\mathcal{G}_{(3)}$. All $\mathcal{G}_{(1)}$–$\mathcal{G}_{(3)}$ are strongly connected and balanced. An *arrow* from j to i denotes that agent j is a neighbor of agent i

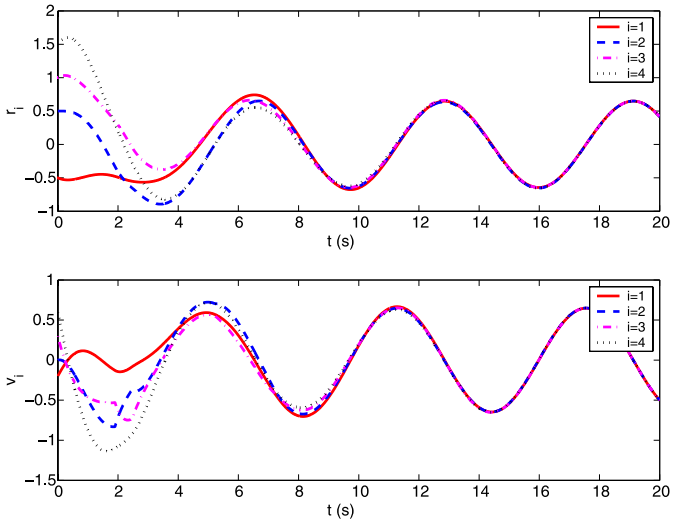

Fig. 3.18 Evolution of the oscillator states using (3.12) when $\alpha_{\sigma(t)} \equiv 1$ and $\mathcal{G}(t)$ switches from $\{\mathcal{G}_{(1)}, \mathcal{G}_{(2)}, \mathcal{G}_{(3)}\}$ as shown in Fig. 3.17

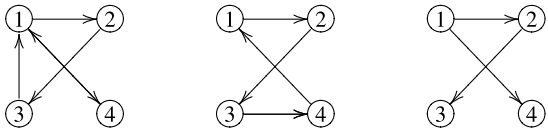

(a) $\mathcal{G}_{(1)}$ (b) $\mathcal{G}_{(2)}$ (c) $\mathcal{G}_{(3)}$

Fig. 3.19 Directed graphs $\mathcal{G}_{(1)}$–$\mathcal{G}_{(3)}$. All of them have a directed spanning tree. An *arrow* from j to i denotes that agent j is a neighbor of agent i

3.2.4 Application to Motion Coordination in Multi-agent Systems

In this subsection, we apply (3.24) to motion coordination in multi-agent systems. Suppose that there are four point-mass agents in the team with dynamics give by $\dot{p}_i = q_i$ and $\dot{q}_i = w_i$, $i = 1, \ldots, 4$, where $p_i \triangleq [x_i, y_i]^T$ is the position, $q_i \triangleq [v_{xi}, v_{yi}]^T$ is the velocity, and $w_i \triangleq [w_{xi}, w_{yi}]^T$ is the acceleration input. Also suppose that there exists a virtual leader, labeled as agent 0, with the position $p_0 \triangleq [x_0, y_0]^T$ and the velocity $q_0 \triangleq [v_{x0}, v_{y0}]^T$, and p_0 and q_0 satisfy

$$\dot{p}_0 = q_0, \qquad \dot{q}_0 = -\alpha p_0, \tag{3.29}$$

where α is a positive constant. We apply (3.24) to design w_{xi} and w_{yi}, respectively, as

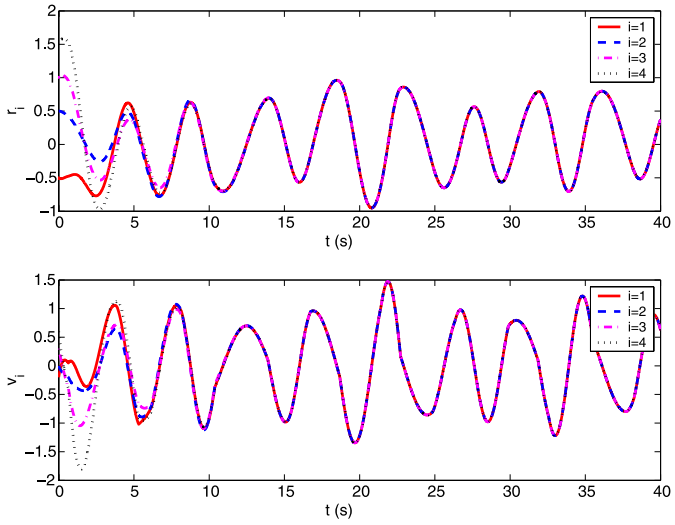

Fig. 3.20 Evolution of the oscillator states using (3.12) when $\alpha_{\sigma(t)}$ switches from (3.28) and $\mathcal{G}(t)$ switches from $\{\mathcal{G}_{(1)}, \mathcal{G}_{(2)}, \mathcal{G}_{(3)}\}$ as shown in Fig. 3.19

Table 3.1 Parameters and initial conditions used in the simulation

$\alpha = 1$
$\delta_{x1} = 0, \delta_{x2} = 4, \delta_{x3} = 0, \delta_{x4} = 4$
$\delta_{y1} = 0, \delta_{y2} = 0, \delta_{y3} = -4, \delta_{y4} = -4$
$x_0(0) = 1, x_1(0) = 1.2, x_2(0) = 0.8, x_3(0) = 1.4, x_4(0) = 0.5$
$y_0(0) = -1, y_1(0) = -1.2, y_2(0) = -0.8, y_3(0) = -0.7, y_4(0) = 1.5$
$v_{x0}(0) = 1, v_{x1}(0) = 0.2, v_{x2}(0) = 0.3, v_{x3}(0) = 0.4, v_{x4}(0) = 0.5$
$v_{y0}(0) = 1, v_{y1}(0) = 0.4, v_{y2}(0) = 0.6, v_{y3}(0) = 0.8, v_{y4}(0) = 1$

$$w_{xi} = -\alpha(x_i - \delta_{xi}) - \sum_{j=0}^{n} a_{ij}(v_{xi} - v_{xj}),$$
$$w_{yi} = -\alpha(y_i - \delta_{yi}) - \sum_{j=0}^{n} a_{ij}(v_{yi} - v_{yj}),$$

where δ_{xi} and δ_{yi} are constant.

Parameters and initial conditions used in the simulation are shown in Table 3.1. By solving (3.29), it is straightforward to show that the trajectory of the virtual leader follows an elliptic orbit.

Figure 3.21 shows the interaction graph for agents 1 to 4 and the virtual leader (i.e., agent 0). We let $a_{ij} = 1, i, j = 0, \ldots, 4$, if $(j, i) \in \overline{\mathcal{E}}$ and $a_{ij} = 0$ otherwise. Figure 3.22 shows the complete trajectories and snapshots of the four agents.

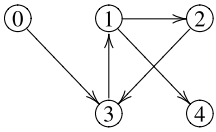

Fig. 3.21 Interaction graph for the four agents and the virtual leader. An *arrow* from j to i denotes that agent j is a neighbor of agent i

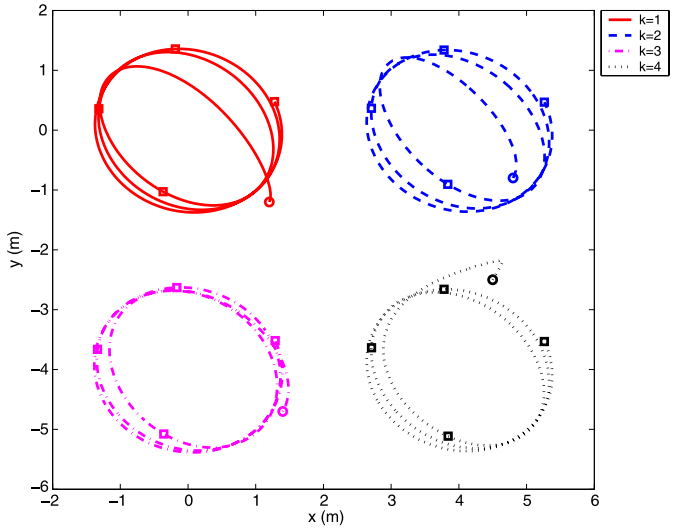

Fig. 3.22 Complete trajectories of the four agents. *Circles* show the snapshot at $t = 0$ s while *squares* show the snapshots at $t = 5, 10, 15, 20$ s

Note that the four agents are able to synchronize their motions and move on elliptic orbits.

3.3 Notes

The results in this chapter are based mainly on [241–244]. For further results on collective periodic motion coordination, see [141, 175, 176, 187, 226, 238, 262, 263, 271, 281]. In particular, a cyclic pursuit strategy, where each agent pursues only one other agent with the interaction graph forming a unidirectional ring, is studied for agents with single-integrator dynamics in [176, 271] while for mobile agents subject to nonholonomic constraints in [187]. The cyclic pursuit strategy is generalized in [226] by letting each agent pursue one other agent along the line of sight rotated by a common offset angle. It is shown that depending on the common offset angle, the agents can achieve different symmetric formations, namely, convergence to a single point, a circle, or a logarithmic spiral pattern in the two-dimensional space.

The result is further extended in [238] to deal with single- and double-integrator models in the three-dimensional space. In particular, it is shown that more robust, locally stable motions on circular orbits can be achieved by making the rotation angle a function of the relative positions of the agents. Symmetric formations are also studied by adopting models based on the Frenet–Serret equations of motion [141] or by exploring the connections between phase models of coupled oscillators and kinematic models of steered particle groups [262, 263]. In addition, a collective rotating formation control problem, where all agents surround a common point with a desired formation structure, is investigated in [175] for double-integrator agents in the two-dimensional space. In [281], synchronization of coupled second-order linear harmonic oscillators is revisited under a dynamic proximity graph. It is shown that the coupled second-order linear harmonic oscillators can always be synchronized without imposing any graph connectivity assumption.